[1,8]. Influenza virus-specific PAMPs are known to be detected by Toll-like receptors (TLR) 3, 7, and 8 [9,10], members of the retinoid acid-inducible gene-I (RIG-I)-like receptors, and Nod-like receptors that recognize viral RNA in the cytoplasm during viral replication [9,11,12]. Stimulation of these receptors triggers induction of type-I interferons (IFNs).

Type-I IFNs, which make up a large family including IFNβ and more than 10 members of IFNα in mammals, share a single receptor IFNα/βR, and play a major role in protecting host cells from viral infections [13]. Type-I IFNs function not only to directly inhibit viral replication, but also to modulate the subsequent immune response by inducing a large number of IFN-inducible molecules, including chemokines [14]. These in turn activate macrophages, dendritic cells, and NK cells, as well as mediate the generation of CTL [15] and antibody-producing cells [16]. Hence, inoculation of live virus or vaccine can modify the activation state and distribution of leukocytes, which may in turn modulate the intensity of virus-specific adaptive immune responses. However, it has not been clarified which particular effect is dependent on the type of vaccine and what viral component induces each host response.

Here we attempted to unravel the mechanisms of these host effects, as induced by either inactivated influenza whole virion vaccine (whole virion) or ether-split vaccine (HA split). Whole virion induces PBL loss concomitant with IFNα production. Mice deficient in IFNα/βR or MyD-88 completely retain PBL after inoculation with whole virion. We further demonstrate that this PBL loss is independent of PBL redistribution, but is instead caused by IFNα-dependent apoptosis of circulating PBL.

2. Materials and methods

2.1. Mice

C57BL/6 (B6) and outbred ddY mice were purchased from Japan SLC and were housed at the National Institute of Infectious Diseases under specific pathogen-free conditions. IFNαβR deficient mice were purchased from B&K Ltd., and backcrossed to the B6 background (B6.IFNα/βR KO) under barrier conditions. MyD-88 deficient mice and TLR7 deficient mice were kindly provided by Dr. Shizuo Akira (Osaka University). All animal procedures were performed in accordance with the guidelines of the Institutional Animal Care and Use Committee, National Institute of Infectious Diseases.

2.2. Influenza virus vaccines

Inactivated influenza whole virion and HA split vaccines were prepared from the vaccine strain A/Wyoming/3/2003 (IVR-134) (H3N2) by the Chemo-Sero-Therapeutic Research Institute, a licensed manufacturer of influenza vaccine in Japan. Briefly, the virus was propagated in the allantoic cavity of embryonated hen's eggs, and pelleted using ultracentrifugation. The pelleted virus was resuspended, further purified by zonal centrifugation with a sucrose density gradient, and inactivated with formalin for the preparation of the whole virion vaccine [17]. To prepare the HA split vaccine, the purified virus was treated with ether and polysorbate 80, and the resulting aqueous solution was recovered [18]. Inactivation was confirmed by the absence of detectable hemagglutination activity following inoculation of the vaccines into embryonated hen's eggs. Each vaccine preparation was formulated to contain a final concentration of immunologically active HA of 90 μg/ml by the use of single-radial-immunodiffusion (SRD) assays.

2.3. Administration of inactivated virus vaccine

Mice were injected i.p. at 6 weeks of age with 500 μl of whole virion or HA split in saline at a concentration of 90 μg/ml HA. For in vivo treatment with pertussis toxin (PTX), mice were injected i.p. with 500 ng of PTX (Sigma–Aldrich) or the same amount of non-functional B-oligomer of PTX (Sigma–Aldrich) as a control on the day before vaccination as previously described [19].

2.4. Flow cytometry

Ten μl of blood from the tail vein was harvested in PBS containing 0.05% heparin (Mochida Pharmaceutical). After erythrolysis by treatment with hypotonic sodium ammonium chloride buffer, the FcγR on PBL were blocked with anti-FcγRII/III mAb (2.4G2), and the cells were stained with fluorescein isothiocyanate (FITC)-labeled anti-B220 (RA3-6B2), phycoerythrin (PE)-labeled anti-CD3ε (2C11), allophycocyanin (APC) or Pacific blue-labeled anti-Ly-6C/G (RB6-8C5) mAb, (eBioSciences), and propidium iodide (PI; Sigma–Aldrich). The absolute PBL number was determined and PBL subsets were analyzed using a FACSCalibur (BD Biosciences). In some experiments, PBL were further stained with APC-labeled annexin-V (BD PharMingen) for detecting apoptotic cells.

2.5. Enzyme-linked immunosorbent assay (ELISA).

Sera from vaccinated mice were collected from the tail vein or by cardiac puncture under anesthesia. The level of cytokines in sera was measured using a Ready-Set-Go! ELISA assay kit (for TNF, IL-1α, IL-12p70; eBioscience) or mouse type-I IFNs ELISA kit (for IFNα and IFNβ; PBL) according to the manufacturers' instructions.

2.6. Anti-influenza virus antibodies

One hundred μl of sera were collected from the tail veins of individual mice at the time points indicated in the text. Anti-influenza virus Ab titers were estimated by ELISA assays using whole virion or HA split vaccine as the coating antigen [20].

3. Results

3.1. Inactivated influenza A virus but not HA split vaccine causes a loss of PBL

First, we investigated the ability of whole virion and HA split, both derived from the same vaccine strain of influenza virus A/Wyoming/3/2003 (IVR-134) (H3N2), to decrease the number of PBL. The HA protein content in each vaccine was standardized using an SRD assay, a potency assay currently used for inactivated influenza vaccine. Fig. 1A shows that the total number of PBL in a 10 μl aliquot of blood was decreased in mice shortly after immunization with the whole virion in a dose-dependent manner, but this effect was not seen with the HA split or saline inoculations ($P < 0.05$). Strikingly, whole virion vaccination induced a dose dependent decrease in the number of T- and B-cells (Fig. 1B and C), and to a lesser extent, granulocytes (Fig. 1D). However, administration of HA split vaccine did not induce a significant decrease of total PBL or any of the subpopulations. The decrease in PBL numbers after inoculation of whole virus particles was seen not only in outbred ddY mice but also in inbred strains such as B6 and BALB/c (data not shown). These findings suggest that the administration of whole virus particles causes a rapid decrease of PBL, as also seen in live influenza virus infection [4,6] and following administration of a viral RNA analog, polyinocinic-polycytidylic acid (poly (I:C)) [21], whereas administration of HA split vaccines do not affect PBL numbers.

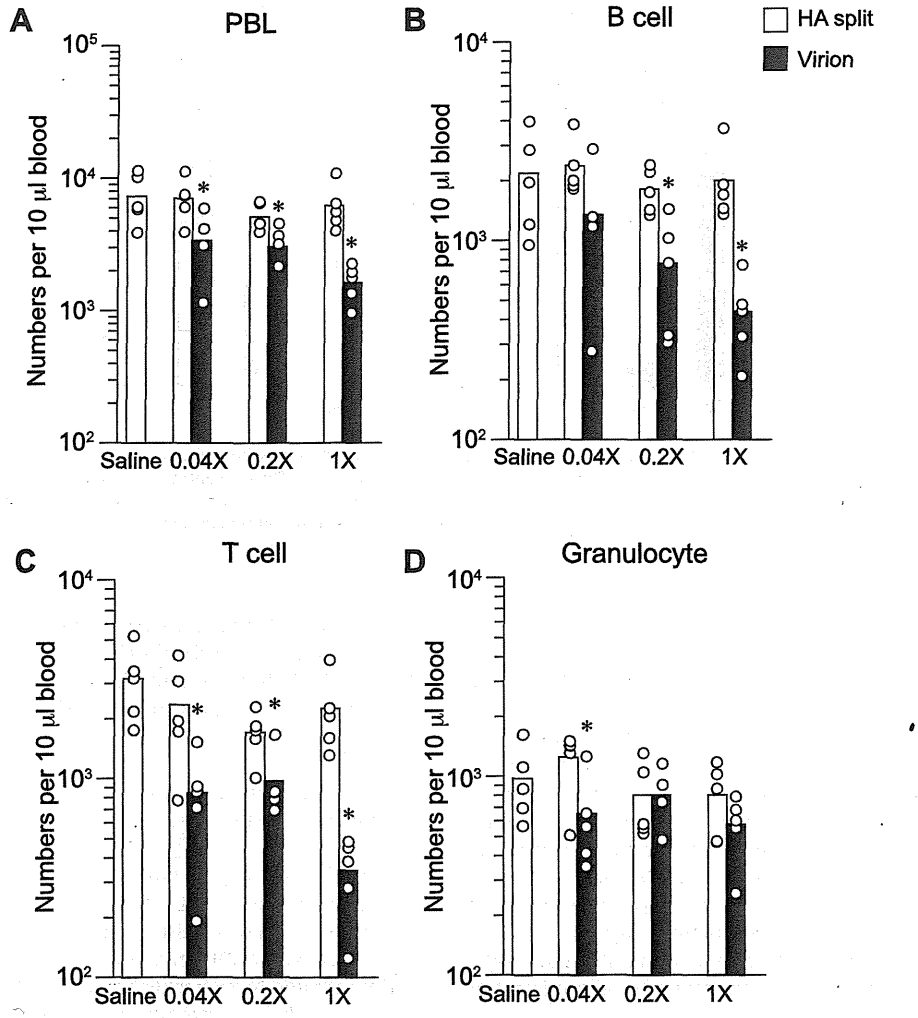

Fig. 1. Effect of inactivated influenza A vaccines on the number of PBL and of leukocyte subsets. ddY mice were injected i.p. with saline, HA split (open column) or inactivated whole virion (closed column) vaccines. The starting dose was 0.5 ml, which had been adjusted to contain the same quantity of immunologically active HA in both vaccines, with a series of dilutions as indicated. Ten μl of blood from the tail vein was collected at 16 h after inoculation. Cells were stained with PI, anti-Gr-1, anti-B220, and anti-CD3 Abs, and analyzed using flow cytometry to identify leukocyte subsets. A summary of the number of peripheral blood leukocytes (PBL) (A), B cells (B), T cells (C), and granulocytes (D) of vaccine- and saline-administrated mice is shown. Dots indicate individual values and columns indicate mean values ($n = 5$). *$P < 0.05$.

3.2. *Ab response to influenza virus is independent of the decrease of PBL*

Next, we examined the influence of PBL loss on acquired immune responses against influenza A virus. We measured the titer of influenza virus-specific antibody in the sera of whole virion-immunized or HA split-immunized mice. As shown in Fig. 2, we evaluated primary Ab responses by ELISA at 10 days, 30 days, and 50 days post immunization with three vaccine doses. There was no significant difference in virus-specific IgG1 titers between whole viral- and HA split- immunized mice (Fig. 2). These data indicate that the HA content measured by SRD assay for determining the vaccine doses correlated well with the in vivo virus-specific Ab responses.

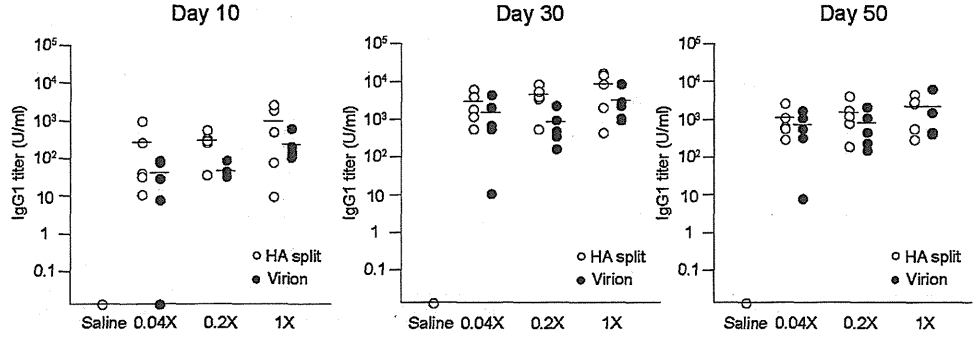

Fig. 2. Anti-influenza virus immune responses induced by immunization with whole virion and HA split vaccines. ddY mice were injected i.p. with HA split (○) and whole virion (●) vaccines with the same condition as in Fig. 1. Sera from peripheral blood were collected on the indicated days post immunization. The titers of IgG1 Abs were measured by influenza virus-specific ELISA. Bars indicate mean values ($n = 5$).

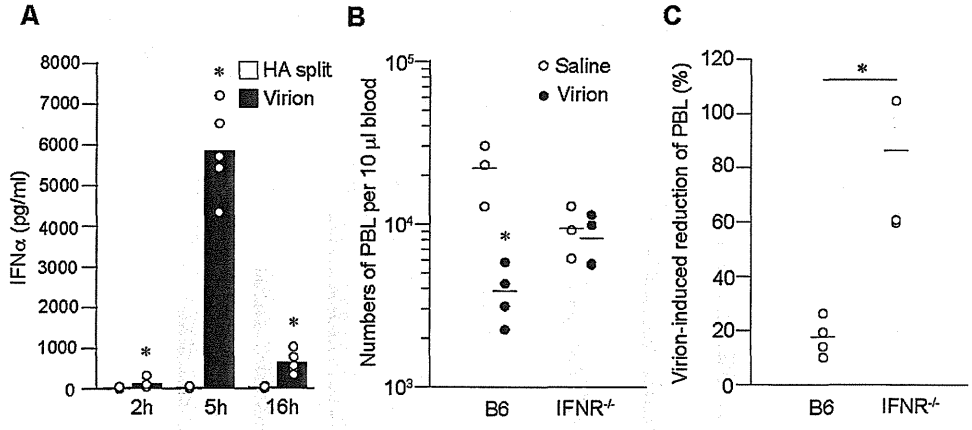

Fig. 3. The increased level of IFNα is responsible for the decreased number of PBL after administration of whole virion vaccine. (A) Sera were collected at the time points indicated from tail veins of mice that were injected i.p. with HA split (○) or whole virion (●) vaccines. The concentration of IFNα was determined by ELISA. Bars indicate mean values ($n=5$) *$P<0.05$. (B) Wild type C57BL/6 mice and B6.IFNα/βR KO mice were injected i.p. with 0.5 ml of saline or inactivated influenza virus; 16 h later, 10 μl of blood was collected from the tail vein. Absolute numbers of PBL (B) and the proportions of PBL in virion-administrated mice to those in mock treated mice (C) are shown. Bars indicate mean values ($n=5$). *$P<0.05$.

3.3. Loss of PBL was correlated with a high level of serum IFNα

Next, we explored which molecule is associated with PBL loss during innate immune response activation. We measured the serum levels of TNF, IL-1α, and IL-12, at 2, 5, and 16 h post inoculation, but we could not detect significant levels of those molecules with either vaccination protocol (data not shown). On the other hand, serum IFNα was detectable at 2 h post inoculation, peaked at 5 h, and was sustained even at 16 h in whole virion administrated mice (Fig. 3A). On the contrary, mice given the HA split vaccine did not produce significant IFNα. The kinetics of IFNβ concentration in sera were similar to those of IFNα (Supplementary Fig. 1). These findings indicate that the increased level of serum IFNα and IFNβ are associated with innate immune responses after administration of whole virions.

In order to evaluate whether the PBL decrease is mediated by IFNα signaling, whole virion vaccine was administrated to mice lacking the IFNα/β receptor gene (B6.IFNα/βR KO mice). Unmanipulated B6.IFNα/βR KO mice had a similar PBL profile as wild type (WT) B6 mice, including T-cell, B-cell, conventional dendritic cells, and plasmacytoid dendritic cells (pDC) in their blood and spleens (data not shown). Fig. 3B and C show that administration of whole virion resulted in a significant reduction in the number of PBL in WT B6 mice but not in IFNα/βR KO mice. These results suggest that the loss of PBL following administration of whole virion is associated with IFNα signaling through the IFNα/βR.

3.4. TLR signaling is necessary for the loss of PBL after inoculation of influenza vaccine

As data on Fig. 3 raise the possibility that innate immune responses are responsible for the decrease of PBL numbers, we tried to define which recognition units mediate the loss of PBL occurring with inactivated influenza virus. To this end, whole virions were administrated to B6 background mice deficient in MyD-88 or TLR7, molecules that are potentially involved in signal transduction of influenza virus-mediated IFNα expression. In contrast to WT mice, which had about an 80% reduction in PBL numbers at 16 h after injection of whole virions, B6.MyD-88 KO mice showed no decrease (Fig. 4B). On the other hand, B6.TLR7 KO mice exhibited a significant but less severe (~60%) PBL reduction (Fig. 4A, C). These results suggest that whole virions cause PBL loss via a MyD-88-dependent pathway, whereas TLR7 partially contributes.

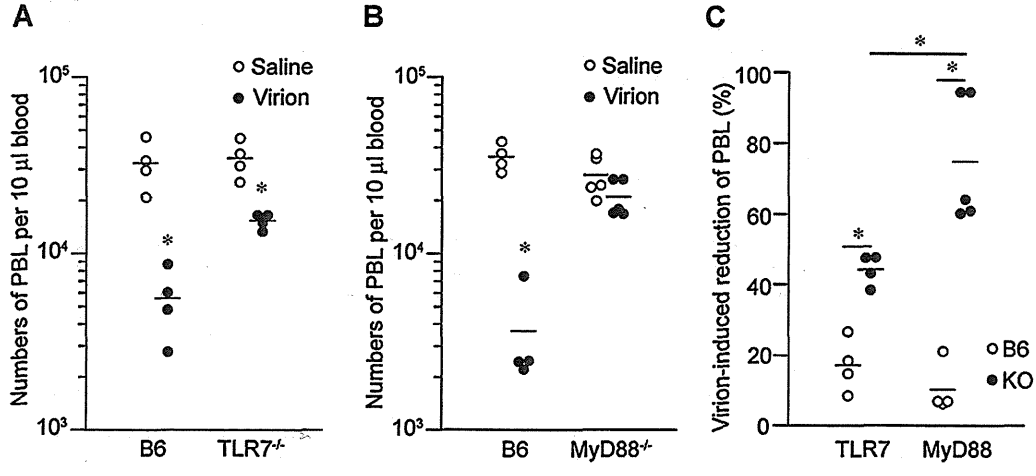

Fig. 4. TLR signaling contributes to the loss of PBL after inoculation with influenza vaccines. C57BL/6 mice, B6.TLR7 KO mice (A), or B6.MyD-88 KO mice (B) were injected i.p. with 0.5 ml of whole virion vaccine. After 16 h, 10 μl of blood was collected from the tail vein and cells were analyzed by flow cytometry. Absolute number of PBL (A, B) and the proportion of PBL in virion-administrated mice to those in mock treated mice (C) are shown. Bars indicate mean values ($n=4$ or 5). *$P<0.05$.

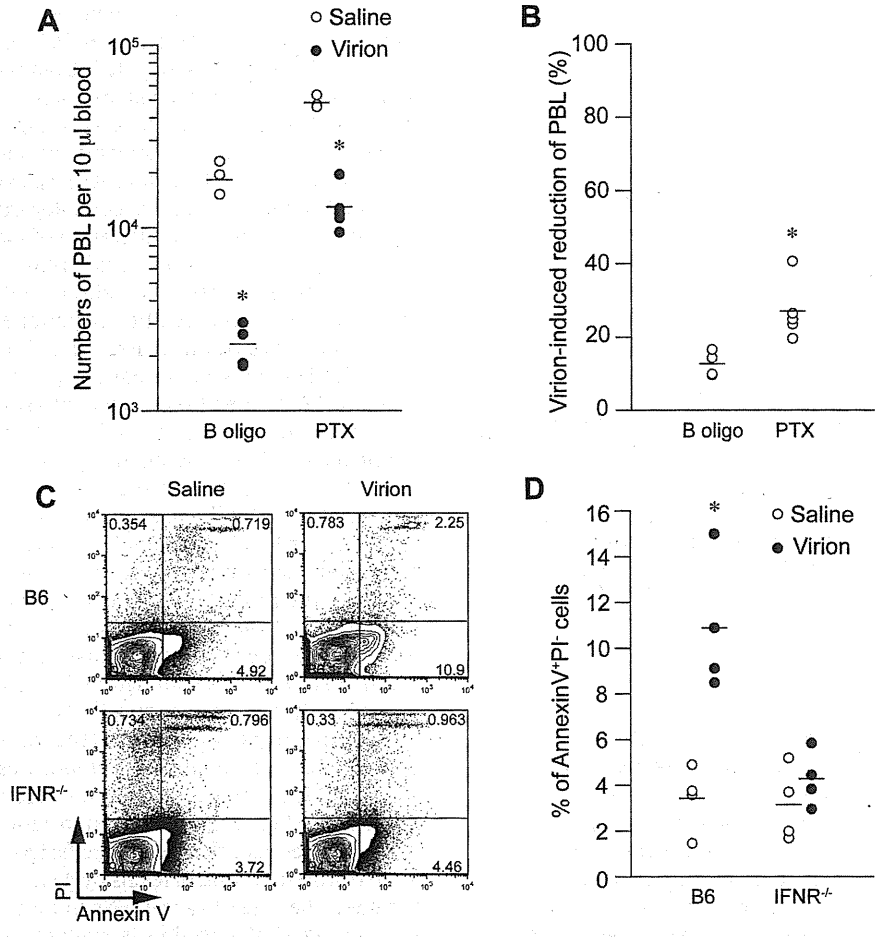

Fig. 5. Loss of PBL by apoptosis but not by redistribution after administration of whole virion. (A, B) C57BL/6 mice were injected i.p. with 0.5 ml of saline (○) or whole virion vaccine (●) along with 500 ng of pertussis toxin or control B oligomer. After 16 h, 10 μl of blood was collected from the tail vein and cells were analyzed by flow cytometry. Absolute PBL number (A) and the proportion of PBL in virion-administrated mice to those in control mice (B) are shown. Bars indicate mean values ($n = 5$). *$P < 0.05$. (C, D) Mice were injected i.p. with 0.5 ml of saline or whole virion vaccine. After 5 h, peripheral blood was collected. Cells were stained with APC-Annexin-V and PI and analyzed by flow cytometry. (C) The numbers in the plots represent the proportion of early apoptotic cells (lower right quadrant) and late apoptotic/necrotic cells (upper right) to total PBL. (D) The proportion of Annexin V^+ PI^- early apoptotic cells in the PBL of saline- (○) or whole virion vaccine- (●) treated wild type C57BL/6 mice and B6.IFNα/βR KO mice. Bars indicate mean values ($n = 5$). *$P < 0.05$.

3.5. Apoptosis is the major mechanism of PBL loss caused by inactivated influenza virus

Next, we approached the underlying mechanisms by which PBL numbers decrease in response to inactivated influenza virus. A previous study has suggested that lymphocytes are trapped in the regional lymph nodes by Sphingosin-1-phosphate (S1P) signaling in the case of live viral infection or poly (I:C) administration [22]. To test this possibility, we administrated PTX, an inhibitor of G protein (Gαi)-coupled receptors for chemokines, including S1P, prior to vaccination of wild type or IFNα/βR KO mice with whole virions. PTX treatment failed to block the PBL decrease in WT mice at 16 h after inoculation of viral particles (Fig. 5A), although the extent of PBL reduction in PTX-treated mice was slightly less than that in the controls (Fig. 5B). These results indicate that GTP-coupled receptors regulating PBL movement do not play a definitive role in the loss of PBL. Therefore, we examined the role of cell death and examined the frequency of apoptosis and necrosis in PBL after administration of whole virions. At 5 h after inoculation, a significant loss of PBL was observed in wild type but not IFNα/βR KO mice (data not shown), which is similar to that seen at 16 h after virus administration (Fig. 3B). Of note, the proportion of Annexin-V^+ positive apoptotic cells was elevated in the PBL from WT mice with virus administration, whereas no significant increase in the apoptotic cell fraction was observed in PBL from B6.IFNα/βR KO mice, or from mock treated mice (Fig. 5C, D). PBL apoptosis was seen at 16 h after inactivated virus inoculation in wild type mice, though the frequency was reduced (Supplementary Fig. 2). Taken together, these data indicate that the loss of PBL after inactivated influenza virus immunization is attributable to apoptosis via IFNα/βR signaling and not to chemoattractant-dependent redistribution.

3.6. Ab response to influenza virus is dependent on IFNα signaling

To evaluate the possible role of IFNα in the establishment of humoral immunity against the influenza vaccine, we further analyzed the ability of IFNα/βR deficient mice to generate virus-specific IgG responses. IgG1 and IgG2c Ab titers were significantly impaired at the early phase after vaccination of B6.IFNα/βR KO mice as compared to wild type mice (Fig. 6, $P < 0.05$). However, at 29 days post vaccination the Ab responses were equivalent in the two mouse strains. These results indicate that IFNα/βR signaling may be necessary for rapid induction of the initial protective IgG response but not to maintain IgG titers against influenza virus.

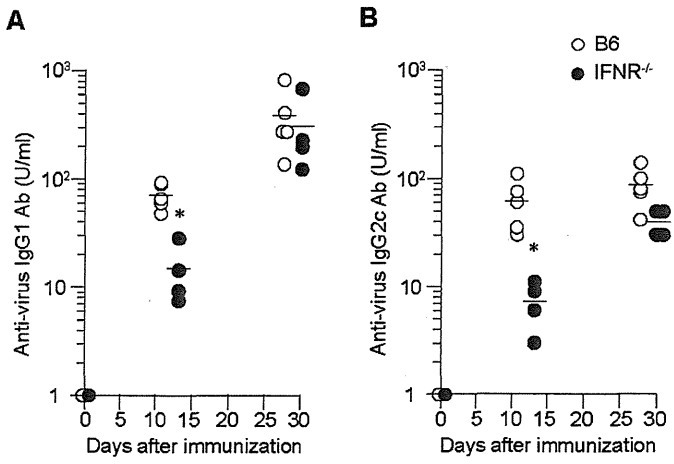

Fig. 6. The role of IFNα signaling in anti-influenza virus IgG responses to whole virion vaccine. Inactivated whole virion was administrated i.p. to wild type C57BL/6 mice (○) and B6.IFNα/βR KO mice (●) using the same conditions as Fig. 2. Sera were collected at days after immunization as indicated. The serum levels of (A) virus-specific IgG1 and (B) IgG2c antibodies were evaluated by ELISA. Bars indicate mean values ($n = 5$). *$P < 0.05$.

4. Discussion

It has been reported that the inactivated whole virion vaccine was much more effective at inducing protective immunity to influenza virus than the ether-split HA vaccine, because the former contains viral ssRNA that can activate innate immunity via TLR-7/8 signaling [23,24]. However, the precise mechanism of vaccine-induced unwanted adverse reactions, which are mainly due to excessive immune responses, is not fully understood. In this study, we immunized mice with two types of available influenza vaccines, whole virion and HA split, adjusted to contain the same quantity of immunologically active HA in both groups. To our knowledge, this is the first study demonstrating that the administration of whole virion, but not the HA split vaccine, has the potential to reduce the number of PBL in a type-I IFN signaling-dependent manner. This phenomenon is not only recognized in mice but could be reproduced in humans, because previous studies have shown that the administration of type-I IFNs or inactivated influenza virus causes a rapid decrease of PBL in both humans [7,25,26] and mice [20,27,28].

PAMPs of influenza virus, which have the ability to induce type-I IFNs, are strong candidates for the factors responsible for PBL loss. We further show that this PBL loss is completely abrogated in MyD-88 KO mice and partially in TLR7 KO mice. Among the components of influenza virus, viral ssRNA is recognized by TLR7. In formalin-inactivated virus, viral ssRNA is probably encapsulated inside the viral particles. By contrast, RNA in HA split is exposed due to the loss of capsid lipids by ether treatment, which may allow RNase in blood to degrade the viral ssRNA before it can be captured by pDCs. Nevertheless, residual undigested RNA in HA split may impact on the intensity of HA-specific Ab responses [29], considering the discrepancy in kinetics between HA split-administrated WT mice and whole virion-administrated B6.IFNα/βR KO mice. This hypothesis will be tested by further examination of PBL loss using a liposome-encapsulated HA split. Of note, partial loss of PBL in TLR7 KO mice suggests that influenza virus stimulates MyD-88-associated signaling by other PRRs. Recently, it has been shown that pDCs from TLR7 KO mice retain the potential to produce IFNα in response to whole virions [23]. Moreover, endocytosed influenza virus ssRNA could be recognized by NOD-like receptor protein 3, which results in inflammasome activation in mice [12]. Collectively, TLR7 in addition to the autocrine/paracrine IL-1β-MyD-88 mediated signal pathway may be necessary for the production of sufficient type-I IFNs necessary to induce leukocytopenia.

Viral infections [2–4] or poly (I:C) administration [21] are known to induce leukocytopenia via production of type-I IFNs, suggesting that a viral PRRs–type-I IFNs axis is responsible for the loss of PBL. However, the precise mechanisms by which type-I IFNs cause acute leukocytopenia and the different role played by each member of the type-I IFN family remain obscure. Regarding the fate of the missing leukocytes after administration of inactivated influenza virus, there are two possibilities: redistribution and cell death. Shiow et al. [22] have reported that administration of poly (I:C) or LCMV infection causes accumulation of peripheral blood lymphocytes in lymph nodes by blocking S1P receptor 1 signaling. However, we and others [28] demonstrated that S1P plays a very limited role in PBL reduction. Additionally, we detected a slight decrease of peripheral blood granulocytes, which is independent of egress from secondary lymph nodes. These discrepancies may be attributed to differences in the focus on leukocyte subsets, in the magnitude of type-I IFN production, and/or the use of different TLR ligands in each system. On the other hand, PBL rapidly undergo apoptosis in a type-I IFN dependent manner prior to the massive reduction of PBL numbers. Although the precise mechanism remains to be elucidated, it has been reported that type-I IFNs cause rapid activation of peripheral T- and B-cells [30], which may lead to activation-induced cell death [31]. Otherwise, antagonistic activity of type-I IFNs to IL-7 may affect lymphocyte survivals [14].

Several groups have reported that the type-I IFN signaling pathway is essential for proper humoral responses to the influenza vaccine [23,32,33]. However, their observations were all made at a relatively short time after immunization: within 1–2 weeks. We demonstrated that the virus-specific IgG titers in IFNα/βR KO mice were restored to control levels by 4 weeks after vaccination. Taken together, the role of type-I IFNs in influenza-specific IgG production during viral infection is evident from the previous studies, but might be overstated and limited to within a short time after vaccination with inactive whole virions.

In summary, the administration of inactivated influenza whole vaccine causes a rapid loss of PBL in an IFNα-dependent manner. The inability of HA-split vaccine to induce IFNα suggests that packaging of viral ssRNA is important for strong induction of innate immunity. The rapid apoptosis of PBL, which include circulating memory lymphocytes, may influence immune responses to other antigens, suggesting that keeping a balance between innate and acquired immunity is required for more appropriate vaccination strategies.

Acknowledgements

We thank for Dr. Shizuo Akira for providing us MyD-88 KO and TLR7 KO mice, Dr. Shinsuke Taki (Shinshu University), Dr. Noriko Sorimachi (National Center for Global Health and Medicine), and Dr. Kiichi Yamamoto (Tokyo Medical and Dental University) for providing us reagents and techniques. We are grateful to Ms. Yoko Nakamura for technical help. This work is supported by Grants from the Ministry of Health, Labor, and Welfare of Japan.

Appendix A. Supplementary data

Supplementary data associated with this article can be found, in the online version, at http://dx.doi.org/10.1016/j.vaccine.2013.02.016.

References

[1] Aoshi T, Koyama S, Kobiyama K, Akira S, Ishii KJ. Innate and adaptive immune responses to viral infection and vaccination. Curr Opin Virol 2011;1:226–32.

[2] Woodruff JF, Woodruff JJ. Virus-induced alterations of lymphoid tissues. I. Modification of the recirculating pool of small lymphocytes by Newcastle disease virus. Cell Immunol 1970;1:333–54.
[3] Nanan R, Chittka B, Hadam M, Kreth HW. Measles virus infection causes transient depletion of activated T cells from peripheral circulation. J Clin Virol 1999;12:201–10.
[4] Tumpey TM, Lu X, Morken T, Zaki SR, Katz JM. Depletion of lymphocytes and diminished cytokine production in mice infected with a highly virulent influenza A (H5N1) virus isolated from humans. J Virol 2000;74:6105–16.
[5] Kurokawa M, Ishida S, Asakawa S, Iwasa S, Goto N. Toxicities of influenza vaccine: peripheral leukocytic response to live and inactivated influenza viruses in mice. Jpn J Med Sci Biol 1975;28:37–52.
[6] Lewis DE, Gilbert BE, Knight V. Influenza virus infection induces functional alterations in peripheral blood lymphocytes. J Immunol 1986;137:3777–81.
[7] Faguet GB. The effect of killed influenza virus vaccine on the kinetics of normal human lymphocytes. J Infect Dis 1981;143:252–8.
[8] Schenten D, Medzhitov R. The control of adaptive immune responses by the innate immune system. Adv Immunol 2011;109:87–124.
[9] Meylan E, Tschopp J, Karin M. Intracellular pattern recognition receptors in the host response. Nature 2006;442:39–44.
[10] Diebold SS, Kaisho T, Hemmi H, Akira S, Reis e Sousa C. Innate antiviral responses by means of TLR7-mediated recognition of single-stranded RNA. Science 2004;303:1529–31.
[11] Kato H, Takeuchi O, Sato S, Yoneyama M, Yamamoto M, Matsui K, et al. Differential roles of MDA5 and RIG-I helicases in the recognition of RNA viruses. Nature 2006;441:101–5.
[12] Ichinohe T, Lee HK, Ogura Y, Flavell R, Iwasaki A. Inflammasome recognition of influenza virus is essential for adaptive immune responses. J Exp Med 2009;206:79–87.
[13] Pestka S, Krause CD, Walter MR. Interferons, interferon-like cytokines, and their receptors. Immunol Rev 2004;202:8–32.
[14] Bogdan C, Mattner J, Schleicher U. The role of type I interferons in non-viral infections. Immunol Rev 2004;202:33–48.
[15] Le Bon A, Etchart N, Rossmann C, Ashton M, Hou S, Gewert D, et al. Cross-priming of CD8+ T cells stimulated by virus-induced type I interferon. Nat Immunol 2003;4:1009–15.
[16] Jego G, Palucka AK, Blanck JP, Chalouni C, Pascual V, Banchereau J. Plasmacytoid dendritic cells induce plasma cell differentiation through type I interferon and interleukin 6. Immunity 2003;19:225–34.
[17] Reimer CB, Baker RS, Newlin TE, Havens ML. Influenza virus purification with the zonal ultracentrifuge. Science 1966;152:1379–81.
[18] Davenport FM, Hennessy AV, Brandon FM, Webster RG, Barrett Jr CD, Lease GO. Comparisons of serologic and febrile responses in humans to vaccination with influenza A viruses or their hemagglutinins. J Lab Clin Med 1964;63:5–13.
[19] Ato M, Nakano H, Kakiuchi T, Kaye PM. Localization of marginal zone macrophages is regulated by C–C chemokine ligands 21/19. J Immunol 2004;173:4815–20.
[20] Takahashi Y, Inamine A, Hashimoto S, Haraguchi S, Yoshioka E, Kojima N, et al. Novel role of the Ras cascade in memory B cell response. Immunity 2005;23:127–38.
[21] Korngold R, Blank KJ, Murasko DM. Effect of interferon on thoracic duct lymphocyte output: induction with either poly I:poly C or vaccinia virus. J Immunol 1983;130:2236–40.
[22] Shiow LR, Rosen DB, Brdicková N, Xu Y, An J, Lanier LL, et al. CD69 acts downstream of interferon-alpha/beta to inhibit S1P1 and lymphocyte egress from lymphoid organs. Nature 2006;440:540–4.
[23] Geeraedts F, Goutagny N, Hornung V, Severa M, de Haan A, Pool J, et al. Superior immunogenicity of inactivated whole virus H5N1 influenza vaccine is primarily controlled by Toll-like receptor signalling. PLoS Pathog 2008;4:e1000138.
[24] Koyama S, Aoshi T, Tanimoto T, Kumagai Y, Kobiyama K, Tougan T, et al. Plasmacytoid dendritic cells delineate immunogenicity of influenza vaccine subtypes. Sci Transl Med 2010;2:25ra24.
[25] Schattner A, Meshorer A, Wallach D. Involvement of interferon in virus-induced lymphopenia. Cell Immunol 1983;79:11–25.
[26] Gillespie JH, Scott FW, Geissinger CM, Czarniecki CW, Scialli VT. Levels of interferon in blood serum and toxicity studies of bacteria-derived bovine alpha$_1$ interferon in dairy calves. J Clin Microbiol 1986;24:240–4.
[27] Degré M. Influence of exogenous interferon on the peripheral white blood cell count in mice. Int J Cancer 1974;14:699–703.
[28] Kamphuis E, Junt T, Waibler Z, Forster R, Kalinke U. Type I interferons directly regulate lymphocyte recirculation and cause transient blood lymphopenia. Blood 2006;108:3253–61.
[29] Jeisy-Scott V, Kim JH, Davis WG, Cao W, Katz JM, Sambhara S. TLR7 recognition is dispensable for influenza virus A infection, but important for the induction of hemagglutinin-specific antibodies in response to the 2009 pandemic split vaccine in mice. J Virol 2012;86:10988–98.
[30] Alsharifi M, Lobigs M, Regner M, Lee E, Koskinen A, Müllbacher A. Type I interferons trigger systemic, partial lymphocyte activation in response to viral infection. J Immunol 2005;175:4635–40.
[31] Manna SK, Mukhopadhyay A, Aggarwal BB. IFN-alpha suppresses activation of nuclear transcription factors NF-kappa B and activator protein 1 and potentiates TNF-induced apoptosis. J Immunol 2000;165:4927–34.
[32] Proietti E, Bracci L, Puzelli S, Di Pucchio T, Sestili P, De Vincenzi E, et al. Type I. IFN as a natural adjuvant for a protective immune response: lessons from the influenza vaccine model. J Immunol 2002;169:375–83.
[33] Coro ES, Chang WL, Baumgarth N. Type I. IFN receptor signals directly stimulate local B cells early following influenza virus infection. J Immunol 2006;176:4343–51.

Jpn. J. Infect. Dis., 65, 19-27, 2012

Original Article

Newly Established Monoclonal Antibodies for Immunological Detection of H5N1 Influenza Virus

Kazuo Ohnishi[1], Yoshimasa Takahashi[1], Naoko Kono[2], Noriko Nakajima[3], Fuminori Mizukoshi[1], Shuhei Misawa[4], Takuya Yamamoto[1], Yu-ya Mitsuki[1], Shu-ichi Fu[1], Nakami Hirayama[1], Masamichi Ohshima[1], Manabu Ato[1], Tsutomu Kageyama[2], Takato Odagiri[2], Masato Tashiro[2], Kazuo Kobayashi[1], Shigeyuki Itamura[2], and Yasuko Tsunetsugu-Yokota[1]*

[1]*Department of Immunology,* [2]*Influenza Virus Research Center, and* [3]*Department of Pathology, National Institute of Infectious Diseases, Tokyo 162-8640; and* [4]*Tsuruga Institute of Biotechnology, Toyobo, Co., Ltd., Fukui 914-8550, Japan*

(Received October 4, 2011. Accepted October 28, 2011)

SUMMARY: The H5N1 subtype of the highly pathogenic (HP) avian influenza virus has been recognized for its ability to cause serious pandemics among humans. In the present study, new monoclonal antibodies (mAbs) against viral proteins were established for the immunological detection of H5N1 influenza virus for research and diagnostic purposes. B-cell hybridomas were generated from mice that had been hyperimmunized with purified A/Vietnam/1194/2004 (NIBRG-14) virion that had been inactivated by UV-irradiation or formaldehyde. After screening over 4,000 hybridomas, eight H5N1-specific clones were selected. Six were specific for hemagglutinin (HA) and had in vitro neutralization activity. Of these, four were able to broadly detect all tested clades of the H5N1 strains. Five HA-specific mAbs detected denatured HA epitope(s) in Western blot analysis, and two detected HP influenza virus by immunofluorescence and immunohistochemistry. A highly sensitive antigen-capture sandwich ELISA system was established by combining mAbs with different specificities. In conclusion, these mAbs may be useful for rapid and specific diagnosis of H5N1 influenza. Therapeutically, they may have a role in antibody-based treatment of the disease.

INTRODUCTION

The highly pathogenic (HP) H5N1 avian influenza virus caused the first outbreak in humans in Hong Kong in 1997. This outbreak resulted in the infection of 18 people and resulted in six deaths (1,2). Thereafter, it was determined that H5N1 avian influenza virus was continuously circulated among geese in Southeastern China. Eventually, it spread to other Southeast Asian countries, where it severely damaged poultry farms (3,4). Subsequent H5N1 outbreaks in humans occurred in China and Vietnam in 2003 and in Indonesia in 2005. The most recent endemic has occurred in Egypt. According to a World Health Organization report, the H5N1 avian influenza virus had infected 565 people and resulted in 331 deaths by August 19, 2011 (5). Therefore, although sporadic, this fatal human infection is persistent and has the potential to cause serious future pandemics.

In humans, infection with HP H5N1 avian influenza virus causes high fever, coughing, shortness of breath, and radiological findings of pneumonia (6-8). In severe cases, rapidly progressive bilateral pneumonia develops, causing respiratory failure and may be responsible for the high mortality associated with this virus. de Jong et al. analyzed human cases of H5N1 infection and found that a high viral load and the resulting intense inflammatory response caused severe symptoms; furthermore, viral RNA was frequently detected in the rectum, blood, and nasopharynx (9). Thus, it is essential to detect HP influenza virus infection early and rapidly in order to provide early interventions that protect patients from devastating respiratory failure that arises from a high viral load. Additionally, early viral detection would facilitate rapid identification of infected patients and prevent unregulated contact with other people.

The present diagnostic standard for HP H5N1 influenza is the presence of the neutralization antibody. However, it takes more than 1 week for H5N1-specific antibodies to develop, and a well-equipped biosafety level 3 (BSL3) laboratory is required for the virus neutralization assay. A simpler method is the hemagglutination-inhibition assay using horse erythrocyte. This method has been widely performed on paired acute and convalescent sera from patients with HP H5N1 influenza virus infections. Although this method has acceptable sensitivity, its specificity has been questioned (7).

Isolating the virus from patient samples is the gold standard for diagnosing an infection; however, this is not always possible. For example, the method of sample preparation and preservation strongly influence the ability to isolate the virus. Moreover, a BSL3 laboratory is essential. At present, the most sensitive and rapid method for initial diagnosis of H5N1 virus infections is by conventional or real-time reverse-transcriptase polymerase chain reaction (RT-PCR). However, this proce-

*Corresponding author: Mailing address: Department of Immunology, National Institute of Infectious Diseases, Toyama 1-23-1, Shinjuku-ku, Tokyo 162-8640, Japan. Tel: +81-3-5285-1111, Fax: +81-5285-1150, E-mail: yyokota@nih.go.jp

dure requires expertise in molecular virology and expensive equipment and reagents. Moreover, because of its high sequence specificity, this approach could fail to identify mutant influenza viruses that continually evolve due to a high mutation rate (8).

For screening suspected H5N1 influenza virus in the field, the ideal approach would be to employ an immunology-based technique that detects viral antigens. Such a method is simple and rapid. However, its sensitivity and specificity depend highly on the antibodies used. Thus, an immunological assay that uses appropriate specific antibodies against H5N1 in combination with specific antibodies against other subtypes of influenza virus or viruses that cause febrile diseases would be useful for screening in areas with endemic influenza-like illness. While there are several rapid influenza virus diagnostic systems available for seasonal influenza (10), few exist for H5N1 influenza. Therefore, we have developed a simple and rapid diagnostic system with high sensitivity and specificity for H5N1 influenza virus.

Influenza virus belongs to the family *Orthomyxoviridae*; its genome consists of a negative-sense, single-stranded RNA with eight segments, each encoding structural and non-structural proteins (11). Influenza A viruses are classified into several subtypes based on the hemagglutinin (HA) and neuraminidase (NA) serotypes. In total, there are 16 HA and 9 NA serotypes. The H5N1 viruses are divided into clades 1 and 2 based on their HA genotypes. Clade 2 has been further subdivided into five sub-clades (12). Clade 1 viruses were predominant in Vietnam, Thailand, and Cambodia in the early phase of the 2004–2005 outbreak, whereas clade 2.1 viruses were endemic in Indonesia at that time (8). These two viruses are the major prototypes for the preparation of prepandemic H5N1 vaccines. We used inactivated purified clade 1 virion [A/Vietnam/1194/2004 (NIBRG-14)] as an immunizing antigen to establish mouse monoclonal antibodies (mAbs) specific for H5N1 influenza virus. Characterization of these mAbs revealed that they could detect H5N1 viruses when used in an immunofluorescence staining assay (IFA), Western blotting analysis, immunohistochemistry, and antigen-capture sandwich ELISA. In addition, the mAbs had significant in vitro neutralization activity against H5N1 viruses, and some broadly detected both clade 1 and 2 viruses.

MATERIALS AND METHODS

Viruses and cell culture: The NIBRG-14 (H5N1) virus, which possesses modified HA and NA genes derived from the A/Vietnam/1194/2004 strain on the backbone of six internal genes of A/Puerto Rico/8/34 (PR8), was provided by the National Institute for Biological Standards and Controls (NIBSC; Potters Bar, UK). A/Indonesia/05/2005 (Indo5/PR-8-RG2), A/Turkey/1/2005 (NIBRG-23), A/Anhui/01/2005 (Anhui01/PR8-RG5) were also obtained from NIBSC. All non-H5N1 strains were obtained from a stockpile of seed vaccines of the Influenza Virus Research Center of the National Institute of Infectious Diseases. The live virus was manipulated in a BSL2 laboratory. To produce and purify the virion, the NIBRG-14 and PR8 viruses were propagated in the allantoic cavity of 10-day-old embryonated hens' eggs and purified through a 10–50% discontinuous sucrose gradient by ultracentrifugation (13). The viruses were then resuspended in phosphate-buffered saline (PBS) and inactivated by ultraviolet (UV) irradiation or by treatment with 0.05% formalin at 4°C for 2 weeks. These preparations were served as the inactivated H5N1 virus fraction. These conditions have been previously shown to completely inactivate H5N1 viruses.

Production of mAbs: Nine-week-old female BALB/c mice (Japan SLC, Shizuoka, Japan) were immunized subcutaneously with 20 μg of UV- or formaldehyde-inactivated NIBRG-14 (H5N1) virus using Freund's Complete Adjuvant (Sigma, St. Louis, Mo., USA). Two weeks later, the mice were boosted with a subcutaneous injection of 5 μg of the inactivated virus emulsified with Freund's Incomplete Adjuvant (Sigma). Three days after the boost, sera from the mice were tested by ELISA to determine the antibody titer against the NIBRG-14 virus. The three mice with the highest antibody titers were given an additional boost 14 days after the first boost by intravenous injection of 5 μg of the inactivated virus. Three days later, the spleens of these three mice were excised, and the spleen cells were fused with Sp2/O-Ag14 myeloma cells using the polyethylene glycol method of Kozbor and Roder (14). The fused cells were cultured on twenty 96-well plates and selected with hypoxiantine-aminopterin-thymidine (HAT) medium. The first screening was conducted by ELISA using formalin-inactivated purified NIBRG-14 (H5N1) and PR-8 (H1N1) virions, which were lysed with 1% Triton X100. The lysates (1 mg/ml) were diluted 2,000-fold with ELISA-coating buffer (50 mM sodium bicarbonate, pH 9.6), and the ELISA plates (Dynatech, Chantily, Va., USA) were coated at 4°C overnight. After blocking with 1% ovalbumin in PBS-Tween (10 mM phosphate buffer, 140 mM NaCl, 0.05% Tween 20, pH 7.5) for 1 h, the culture supernatants of the HAT-selected hybridomas were added and incubated for 1 h. After washing with PBS-Tween, the bound antibodies were detected using alkaline phosphatase-conjugated anti-mouse IgG (1:2,000; Zymed, South San Francisco, Calif., USA) and *p*-nitrophenyl phosphate, which served as a substrate. In this first screening, hybridomas that reacted to the H5N1 virus (NIBRG-14) but not to the H1N1 virus (PR-8) were selected.

Baculoviral expression of recombinant HA and NA: Recombinant HA (rHA) and NA (rNA) proteins were produced as previously described (13). Briefly, the HA- and NA-coding genes of NIBRG-14 were amplified by PCR to attach a 6x-His tag to the C terminus of HA and to the N terminus of NA. The amplified DNAs were then cloned into pBacPAK8 (Clontech, Mountain View, Calif., USA) and transfected into Sf-21 (*Spodoptera frugiperda*) insect cells. Recombinant baculoviruses containing the rHA and rNA genes were isolated were used to infect Sf-21 cells. The recombinant proteins tagged with 6x-His were purified with TALON columns (Clontech) according to the manufacturer's protocol.

Neutralization assay: For the neutralization assay, 100 $TCID_{50}$ of H5N1 virus, a standard tissue culture infectious dose for such assays, was incubated for 30 min at 37°C in the presence or absence of the purified mAbs, which had been serially diluted twofold. The viruses

were then added to MDCK cell cultures that had been grown to confluence in a 96-well microtiter plate. The virus strains used were A/Vietnam/1194/2004 (NIBRG-14) (H5N1) (clade 1), A/Indonesia/05/2005 (Ind05/PR8-RG2) (H5N1) (clade 2.1), A/Turkey/1/2005 (NIBRG-23) (H5N1) (clade 2.2), and A/Anhui/01/2005 (Anhui01/PR8-RG5) (H5N1) (clade 2.3). After 3–5 days, the cells were fixed with 10% formaldehyde and stained with crystal violet to visualize the cytopathic effects induced by the virus (15). Neutralization antibody titers were expressed as the minimum concentration of purified immunoglobulin that inhibited a cytopathic effect.

Western blot analysis: UV-inactivated purified H5N1 virus (0.5 μg/lane) was loaded on SDS-PAGE gels under reducing conditions. The proteins were then transferred to a PVDF membrane (Genetics, Tokyo, Japan). After blocking with BlockAce reagent (Snow Brand Milk Products Co., Tokyo, Japan), the membranes were detected with the mAbs or diluted sera (1:1,000) that had been obtained from mice immunized with UV-irradiated H5N1 virus. After washing, the membrane was reacted with the peroxidase-conjugated $F(ab')_2$ fragment of anti-mouse IgG (H + L) (1:20,000; Jackson ImmunoResearch, West Grove, Pa., USA), and the bands were visualized on X-ray film (Kodak, Rochester, N.Y., USA) with chemiluminescent reagents (Amersham Biosciences, Piscataway, N.J., USA).

Purification and biotinylation of mAbs: Hybridomas were grown in Hybridoma-SFM medium (Invitrogen, Carlsbad, Calif., USA) supplemented with recombinant IL-6, penicillin (100 U/mL), and streptomycin (100 μg/mL) (16). The culture supernatants were harvested, and 1/100 volume of 1 M Tris-HCl (pH 7.4) and 1/500 volume of 10% NaN_3 were applied directly on a Protein G-Sepharose 6B column (Amersham Biosciences). The column was washed with PBS and eluted with glycine/HCl (pH 2.8). After measuring the OD_{280} of the fractions, the protein-containing fractions were pooled, and an equal volume of saturated $(NH_4)_2SO_4$ was added. The precipitated proteins were dissolved in PBS, dialyzed against PBS, and stored at −20°C. The purified antibodies were biotinylated with sulfo-NHS-LC-biotin (Pierce, Rockford, Ill., USA) according to the manufacturer's protocol.

Antigen-capture ELISA: The purified antigen-capturing mAb was immobilized on a microplate (Immulon 2; Dynatech) by incubating 4 μg/mL of the mAb in 50 mM sodium bicarbonate buffer (pH 8.6) at 4°C overnight. The microplate was blocked with 1% BSA, washed with PBS-Tween, and reacted with serial dilutions of UV-inactivated purified H5N1 virus for 1 h at room temperature. After washing with PBS-Tween, biotinylated probing mAb (0.1 μg/mL) was added to the wells for 1 h at room temperature. After washing, horseradish peroxidase (HRP)-labeled streptavidin (Zymed) was added to the wells for 1 h at room temperature. After washing, 0.4 mg/mL *o*-phenylenediamine (OPD Sigma P-8412) in OPD Buffer (0.05 M citrate-phosphate buffer pH 5.0, 0.04% H_2O_2) or TMB(+) substrate (DAKO, Kyoto, Japan) was added. The reaction was stopped by adding 2N H_2SO_4, and the OD_{490} or OD_{450} was measured using a multi-well plate reader (Flow Laboratories Inc., Inglewood, Calif., USA).

Immunohistochemistry: Lung tissues were harvested from mice infected with A/Vietnam/1194/2004 (NIBRG-14) or A/HongKong/483/97 (HK483). In addition, autopsied lung tissues of patients infected with influenza virus (H1N1 or 2009 H1N1pdm) were used. Formaldehyde- or formalin-fixed paraffin-embedded lung tissue sections were deparaffinized with xylene and graded ethanol and then autoclaved in 0.1 M citrate-buffer (pH 6.0) at 121°C for 10 min to retrieve the antigens. Endogenous peroxidase was inactivated with 0.3% hydrogen peroxide for 30 min at room temperature. After blocking with M.O.M. blocking reagent (Vector laboratories, Burlingame, Calif., USA) or 5% goat serum, the sections were incubated with each of the mouse mAbs or rabbit polyclonal antibody against type A influenza nucleoprotein at 4°C overnight. After washing off the excess antibodies, the sections were incubated with HRP-labeled anti-mouse IgG followed by tyramide signal amplification system (Biotin-free catalyzed amplification system, CSAII; DAKO) or biotinylated anti-rabbit IgG followed by streptavidin/HRP (LSAB kit; DAKO). The labeled peroxidase activity was detected using diaminobenzidine (DAB; Dojin, Kumamoto, Japan) in 0.015% hydrogen peroxide/0.05 M Tris-HCl (pH 7.6). The sections were counterstained with hematoxylin.

RESULTS

Generation of H5N1-specific mAbs: To establish hybridomas that secrete mAbs specific for the H5N1 virus, BALB/c mice were immunized with the whole virion fraction of purified A/Vietnam/1194/2004 (NIBRG-14) virus. The virus had been inactivated by conventional formaldehyde-fixation or by UV-irradiation to avoid possible changes in antigenicity caused by aldehyde fixation. A standard immunization protocol was used, where mice were boosted twice at 2-week intervals with antigen emulsified first in Freund's Complete Adjuvant and then in Freund's Incomplete Adjuvant. Three days after the final boost, a cell suspension was prepared from the spleens of three immunized mice and fused with SP-2/O myeloma using a polyethylene-glycol method. The fused cells were then selected with HAT (14). Hybridoma screening yielded eight hybridoma clones that reacted to NIBRG-14 lysate but not PR-8 lysate in ELISA (Table 1). Of these clones, seven were from mice immunized with UV-inactivated virion, and one was from mice immunized with formaldehyde-inactivated virion. Six clones (Niid_H5A, Niid_H5B, Niid_H5C, Niid_H5D, Niid_H5E, and Niid_H5F) reacted to rHA protein from a H5N1 virus (recHA_H5N1), while one clone (Niid_N1A) reacted to rNA protein from a H5N1 virus (recNA_H5N1). The remaining clone (Niid_150KA) did not react to either recHA_H5N1 or recNA_H5N1 by ELISA but did react to a 150-kDa molecule on Western blot analysis (described below). Interestingly, seven of the eight clones were from the mice immunized with UV-inactivated virus. The eight hybridomas were successfully cloned by a repeated limiting-dilution method and adapted to a serum-free hybridoma culture medium. The purified antibodies from each clone were biotinylated and used for further experiments.

Table 1. Summary of the eight H5N1-specific mAbs generated in this study

Clone name	Old name	Ig-subclass	ELISA				Western blot	IFA	Histology	Neutralization (μg/mL)	Hemagglutination inhibition
			H5N1_ NIBRG-14	H1N1_ PR-8	recHA_ H5N1	recNA_ H5N1					
Niid_H5A[1)]	YH-1A1	IgG2a	+++	−	+	−	57 kDa	++		1.5 (Clade-dep)	−
Niid_H5B[1)]	YH-2F11	IgG2a	+++	−	+++	−	57 kDa			25	+
Niid_H5C[1)]	OM-A	IgG2a	+++	−	++	−	57 kDa		+(mo/hu)	12	
Niid_H5D[1)]	OM-B	IgG2a	+++	−	++	−	57 kDa		+(mo)	12	
Niid_H5E[1)]	OM-C	IgG2a	+++	−	++	−	57 kDa			12 (Clade-dep)	
Niid_H5F	AY-2C2	IgG1	+++	−	++	−	ND	++		6	−
Niid_N1A[1)]	YH-2D3	IgG2a	+++	−	−	+	ND	++			
Niid_150KA[1)]	OM-D	IgG1	+++	−	−	−	150 kDa	++			−

[1)]: Clones derived from mice immunized with UV-inactivated virus. The remaining clone is derived from a mouse immunized with formaldehyde-inactivated virus.

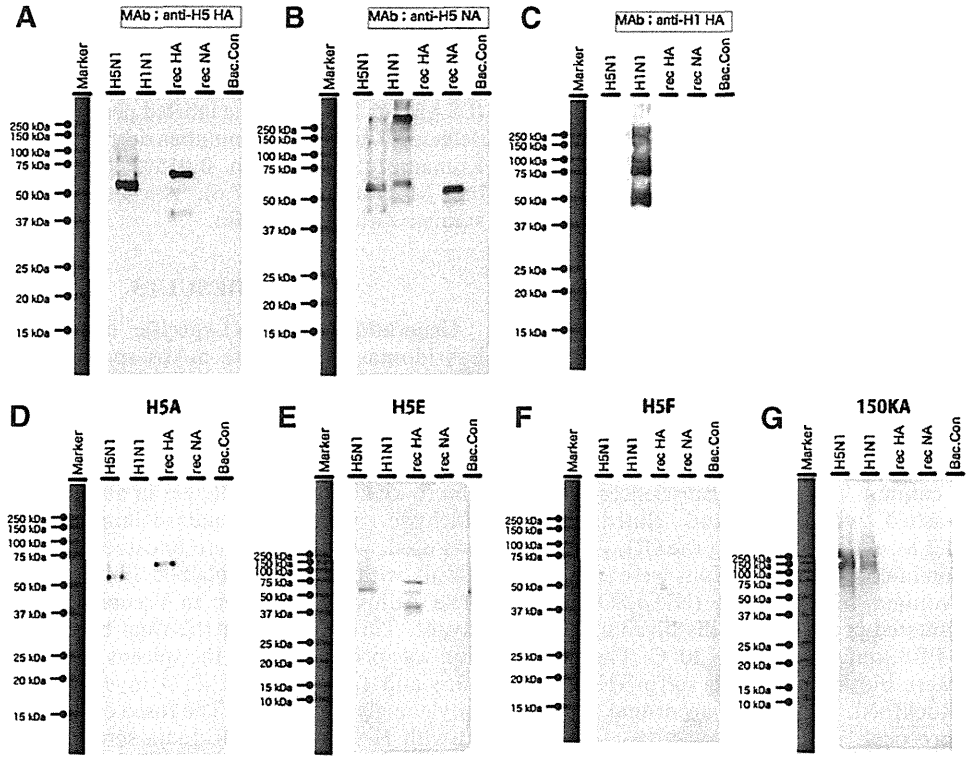

Fig. 1. Detection of influenza virus proteins in Western-blot analysis. Purified influenza virus proteins (0.5 μg/lane) were subjected to SDS-PAGE under reducing conditions. After blotting on a PVDF membrane, the proteins were detected by incubation with the eight monoclonal antibodies (mAbs), followed by incubation with the peroxidase-labeled F(ab')$_2$ fragment of donkey anti-mouse IgG. The mAbs were then visualized by chemiluminescent reaction. A, authentic anti-H5_hemagglutinin mAb; B, authentic anti-H5_neuraminidase mAb; C, authentic anti-H1_ hemagglutinin mAb; D, Niid_H5A; E, Niid_H5E; F, Niid_H5F; G, Niid_150KA. The molecular weight markers are shown on the left.

Western blot analyses with the mAbs: Five mAbs (Niid_H5A, Niid_H5B, Niid_H5C, Niid_H5D, Niid_ H5E) detected the 57-kDa H5_H1 protein by Western blot analysis, which suggests that the antibodies detected the linear epitope(s) of a HA1 fragment of H5_HA (Table 1 and Fig. 1). These antibodies also detected the 60-kDa recombinant H5-HA containing the His-tag. One of these clones, Niid_H5E, detected a 40-kDa subfragment of recombinant HA1, which suggests that the antigenic footprint detected by the mAb differs from that of the other four clones (Fig. 1). Niid-H5F, which reacted strongly to NIBRG-14 and rHA (H5) in ELISA, did not react to any proteins by Western blot analysis, presumably because the mAb detects a conformational epitope of H5-HA. The remaining clone, Niid_150KA, detected an unknown high molecular weight protein of approximately 150 kDa.

IFA with mAbs: Upon IFA, the HA-specific mAbs Niid-H5A and Niid_H5F, the NA-specific mAb Niid-N1A, and the Niid_150KA mAb that detects an

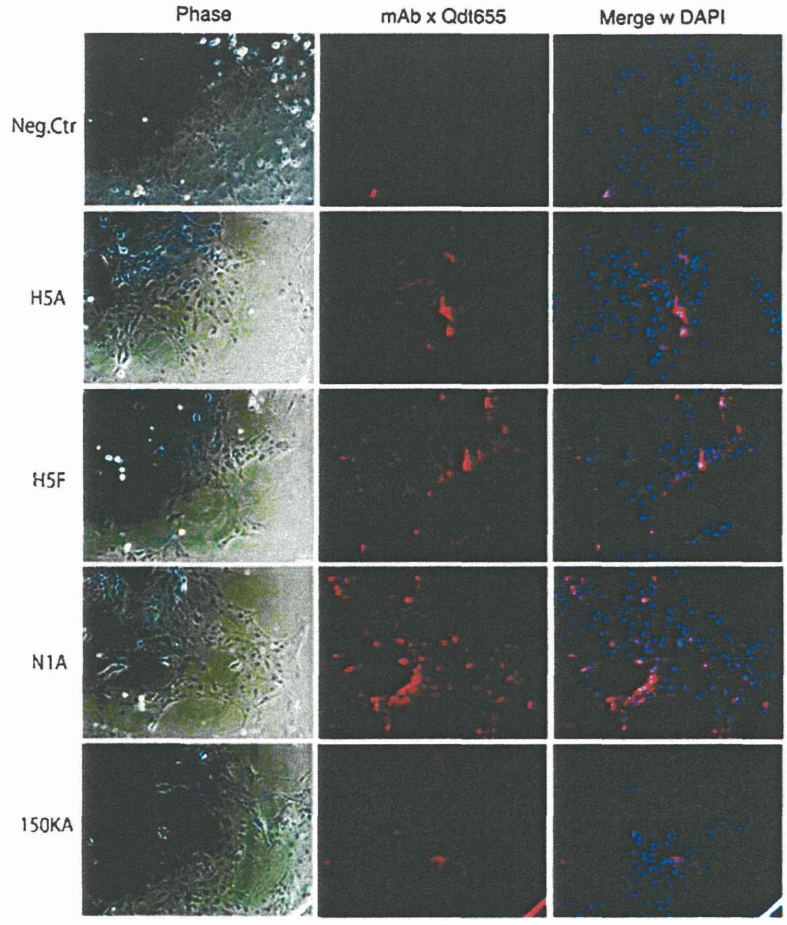

Fig. 2. Fluorescent immunostaining of H5N1 virus-infected MDCK cells with monoclonal antibodies (mAbs). Paraformaldehyde-fixed, H5N1 virus-infected MDCK cells were permeabilized by TBS-Tween and incubated with biotinylated mAbs. The mAbs were detected with Qdot655-conjugated streptavidin (red). Shown are representative staining patterns with Niid_H5A, Niid_H5F, Niid_N1A, and Niid_150KA. The negative control staining without mAb is shown on top. The nuclei were counterstained with DAPI (blue).

unknown 150-kDa protein bound to NIBRG-14-infected MDCK cells (Fig. 2). With the exception of Niid_H5F, these mAbs detected both the perinuclear region and the cell surface of NIBRG-14-infected MDCK cells. Niid_H5F did not detect the perinuclear region (presumably the Golgi body), which suggests that the antigenic footprint detected by this mAb differs from those of the other mAbs.

Immunohistochemistry: The Niid_H5C and Niid_H5D mAbs detected influenza virus antigens in the epithelial cells of the bronchioles and alveoli of 4% formaldehyde-fixed, paraffin-embedded lung tissue sections from mice infected with A/Vietnam/1194/2004 (NIBRG-14) (Fig. 3a). However, none of the mAbs detected influenza virus antigen in lung tissue sections from mice infected with A/HongKong/483/97 (HK483) (Fig. 3). In contrast, a polyclonal antibody against type A influenza nucleoprotein detected type A influenza virus nucleoprotein in the tissue sections from both the NIBRG-14- and HK483-infected mice (Fig. 3b, d). Thus, Niid_H5C and Niid_H5D specifically detected the HA antigen of A/Vietnam/1194/2004 (NIBRG-14). The specificity of these mAbs was then examined by using autopsied lung tissue sections from patients infected with seasonal influenza virus (H1N1) or 2009 pandemic influenza virus (2009H1N1pdm). Niid_H5C did not exhibit any crossreactivity, but the Niid_H5D mAb did show non-specific staining with the human lung section. Two other mAbs, Niid_H5B and Niid_N1A, were also subjected to such immunohistochemical analysis but did not show any reaction.

Neutralization assay with mAbs: The ability of the mAbs to neutralize several H5N1 influenza strains was then tested (Table 2). The four purified H5N1 virus strains, NIBRG-14, Indo-RG2, NIBRG-23, and Anhui-RG5, were diluted to 2–3 $\times$ 10^2 $TCID_{50}$/0.05 mL (Table 2, lower panel) and incubated with titrated amounts of anti-H5_HA mAbs. The remaining infectivity was then noted (Table 2, upper panel). Niid_H5A most potently neutralized the NIBRG-14 strain; it completely neutralized influenza virus infectivity at a concentration of 78 ng/mL. However, Niid_H5A was less potent in neutralizing the Indo-RG2 and Anhui-RG5 strains, which indicates that the neutralizing ability of this mAb was clade-dependent. In contrast, Niid_H5F and Niid_H5D exhibited relatively broad neutralizing abilities, since they neutralized all of the strains that were tested. Niid_H5C and Niid_H5E also showed characteristic clade-

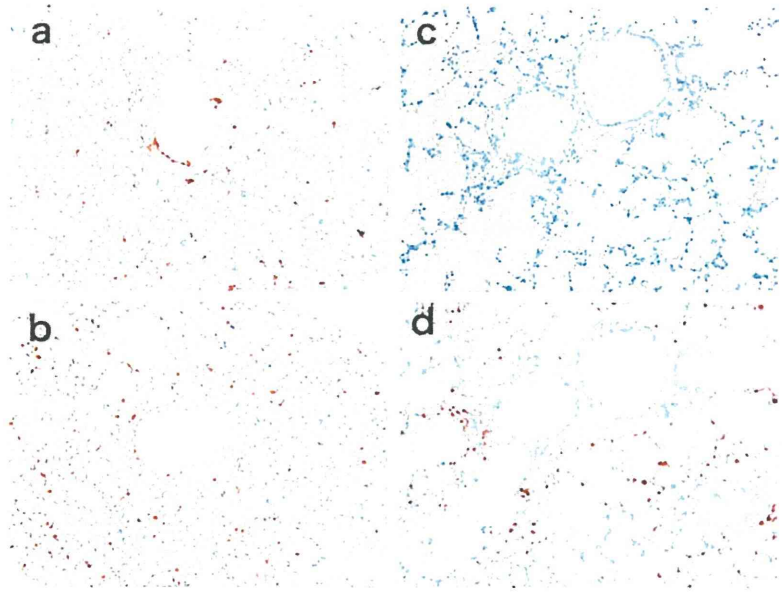

Fig. 3. Immunohistochemical analyses of lung sections from mice infected with A/Vietnam/1194/2004 (NIBRG-14) or A/HongKong/483/97 (HK483) virus. (a, b) Influenza virus antigens were detected in the epithelial cells of the bronchioles and alveoli of the mouse infected with A/Vietnam/1194/2004 (NIBRG-14) by the Niid_H5C clone (a) and polyclonal antibody against type A influenza nucleoprotein (b). (c, d) Virus antigens were not detected in the lung tissue section of the mouse infected with A/HongKong/483/97 (HK483) when Niid_H5C was used (c). However, virus antigens were detected in this section when a polyclonal antibody against type A influenza nucleoprotein was employed (d).

Table 2. Neutralizing ability of the eight mAbs generated in this study

Clone	Neutralizing antibody titer (ng/mL)			
	NIBRG-14 (clade 1)	Indo-RG2 (clade 2.1)	NIBRG-23 (clade 2.2)	Anhui-RG5 (clade 2.3)
Niid_H5A	78	>10,000	625	>10,000
Niid_H5C	625	625	313	>10,000
Niid_H5D	625	625	313	5,000
Niid_H5E	625	>10,000	>10,000	>10,000
Niid_H5F	313	313	156	2,500

Test no.	Virus infection index (Log_{10} $TCID_{50}$/0.05 mL)			
	NIBRG-14	Indo-RG2	NIBRG-23	Anhui-RG5
1	2.5	3.1	2.4	2.1
2	2.0	NT	2.0	2.4

The in vitro neutralization assay examined the ability of the mAbs to neutralize H5N1 virus infection of cultured MDCK cells. Briefly, purified H5N1 virus was diluted to 2-3 $\times$ 10^2 $TCID_{50}$/0.05 mL (the quantities are shown in the lower table) and incubated with serially-titrated purified mAbs for 1 h at 37°C. The samples were then placed into 96-well plates in which MDCK cells had been grown to 90% confluence. After 48 h, the cytotoxicity of the mAb-treated viruses was visualized by staining the cells with crystal violet.
NT, not tested.

dependency, suggesting that the epitopes of these mAbs differ. Interestingly, the mAbs were least able to neutralize Anhui-RG5. This may reflect the genetic distance between Anhui-RG5 (clade 2.3) and NIBRG-14 (clade 1).

Antigen-capture ELISA: To quantitatively detect H5N1 virus, we constructed a sandwich ELISA-based virus antigen-capture detection system. Preliminary experiments tested all combinations of two mAbs from the eight mAbs; Niid_H5F had the highest detection sensitivity for purified H5N1 virion and reacted broadly to the H5_HA of viruses belonging to clades 1, 2.1, 2.2, and 2.3. Therefore, Niid_H5F was selected as the antigen-capturing mAb. The antigen-capture ELISA was constructed by immobilizing Niid_H5F (and/or Niid_H5C) on the ELISA plate and using biotinylated Niid_H5D as the detection mAb, since this combination gave the best results (data not shown). Since the eight mAbs

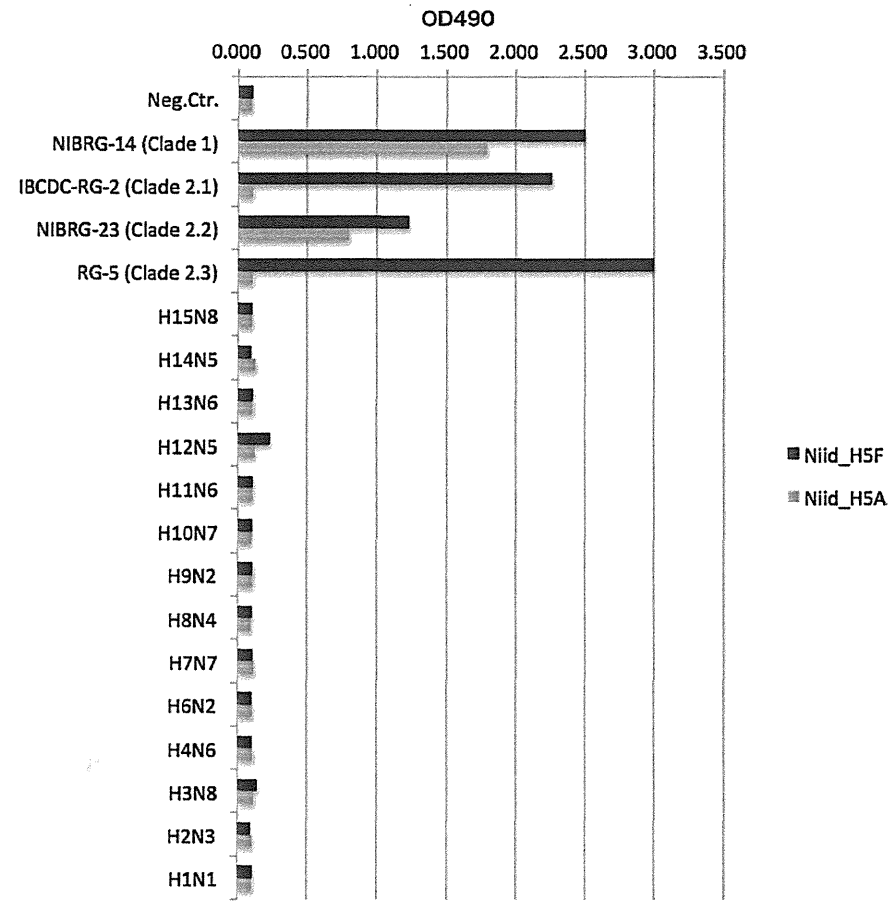

Fig. 4. ELISA reactivity of the Niid_H5A and Niid_H5F monoclonal antibodies (mAbs) to various influenza virus strains. Different influenza virus strains were immobilized on 96-well plates and incubated with biotinylated Niid_H5A or Niid_H5F mAbs followed by peroxidase-labeled streptavidin. The binding of the mAbs was then quantitated by a colorimetric assay using TMB as a substrate.

were originally raised against the H5N1 virus strain A/Vietnam/1194/2004 (NIBRG-14), the validity of this system with other strains of H5N1 virus was also examined. As shown in Fig. 4, this system could detect the A/Indonesia/05/2005 (Indo5/PR-8-RG2), A/Turkey/1/2005 (NIBRG-23), and A/Anhui/01/2005 (Anhui01/PR8-RG5) strains but none of the non-H5N1 strains. The sandwich ELISA could detect H5N1 virus protein at concentrations as low as 50 ng/mL HA, namely, >3 SD of negative samples (Fig. 5).

DISCUSSION

In the present study, mAbs against H5N1 influenza virus were established. These mAbs could detect the virus when used in Western blot analyses, IFA, immunohistochemical analyses, neutralization assays, and antigen-capture ELISA. The characteristics of the mAbs are summarized in Table 1.

Of the eight mAb clones that reacted to H5N1 virus in ELISAs, six reacted to rHA. Only one clone reacted to NA protein. Another clone detected an unknown 150-kDa molecule upon Western blot analysis. A hybridoma that secreted a mAb that could detecte the nuclear protein or other protein components of H5N1 virus was not detected, presumably because the first screening step identified H5 specificity. These results indicate that the HA protein is a dominant target in the antibody response of HA-subtype specificity, as suggested by other studies (17,18). There is accumulating evidence that the influenza strain-specific epitopes are often localized on the HA1 region, whereas the epitopes that are conserved among various strains are localized on the HA2 region (19–22). It has been reported that the immune response elicited by H1N1pdm yields a high frequency of HA2-specific mAbs (23,24). In the present study, none of the established clones detected the HA2 fragment of H5HA, presumably because this study focused on H5-specific clones.

The mAbs isolated in the present study were assessed for their ability to detect H5N1 virus-infected MDCK cells in IFA. Indeed, the anti-HA and anti-NA mAbs detected the cytoplasmic Golgi-rich region and the cell surface membrane. This reflects the common assembly process of influenza virus (25).

In general, a single diagnostic test is not reliable because of the potential for false positives and negatives. Considering the restricted availability of RNA detection systems (26,27), serological screening systems other than those that detect antibodies are currently being ex-

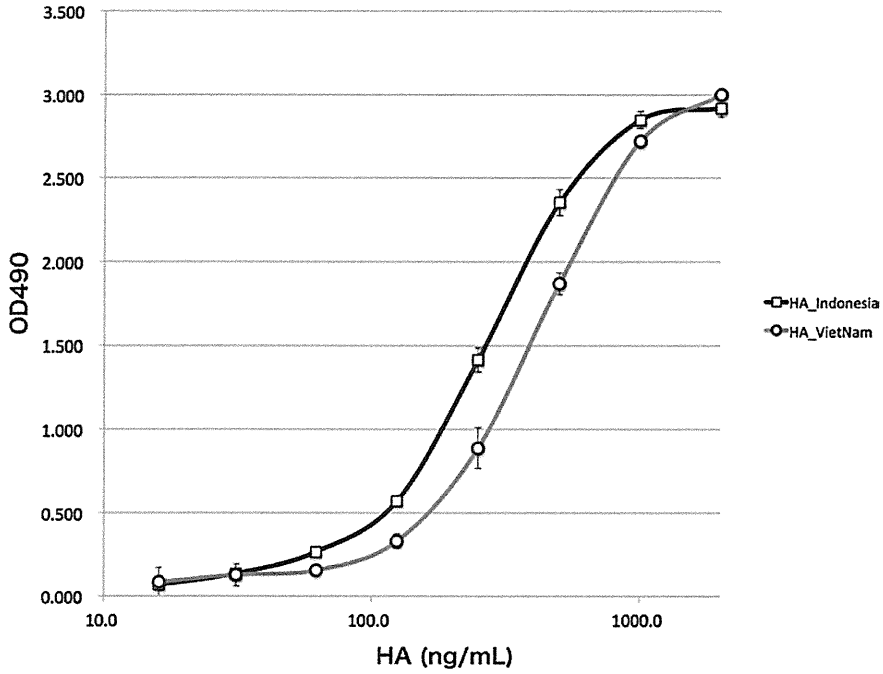

Fig. 5. Antigen-capture ELISA reactivity of monoclonal antibodies (mAbs) to H5N1 and H1N1 virus strains. The anti-H5 mAb Niid_H5F was immobilized on 96-well plates and reacted with serially-titrated purified H5N1 virus fractions for 1 h at room temperature. The bound virus proteins were detected by incubation with biotinylated Niid_H5D (anti-H5) antibody followed by peroxidase-labeled streptavidin. The binding was quantitated by a colorimetric assay that used TMB as a substrate. Abscissa, concentration of purified H5N1 virus proteins. Ordinate, absorbance unit (OD490).

amined. ELISA-based antigen-capture assays offer high specificity and reproducibility and have been used to diagnose and monitor many diseases. The present study describes the development of an antigen-capture ELISA system that detects purified H5N1 virus virion at levels as low as 50 ng/mL. The sensitivity of this system, which comprises three anti-HA mAbs, appears sufficiently high to detect virus protein in patient sera, particularly since a recently reported antigen-capture ELISA system detects 50 ng/mL of purified recombinant HA1 protein (28). At present, the sensitivity of the system is being improved, and its usefulness in diagnosing and monitoring H5N1 virus infections is being validated.

The five selected anti-HA mAbs exhibited significant neutralization activity against several viral strains in a clade-dependent manner (Table 2). Of these, Niid_H5F showed the broadest spectrum of neutralization activity, but it neutralized NIBRG-23 (clade 2.2) more efficiently than the original immunogen NIBRG-14 (clade 1). It would be of interest to determine the features that determine this clade-dependency of mAb recognition. It is also possible that these mAbs have therapeutic potential, if humanized by means of complementarity determining region grafting or mouse-human chimerism.

In conclusion, eight new H5N1-specific mAbs were generated from A/Vietnam/1194/2004 (NIBRG-14)-hyperimmunized mice, six of which were HA-specific. These mAbs were useful in Western blot analyses, IFA, and immunohistology and had in vitro neutralization activity against H5N1 viruses. These mAbs also perform well in a highly sensitive antigen-capture sandwich ELISA system. As such, these mAbs may be useful for the rapid and specific diagnosis of H5N1 subtype influenza virus and may have therapeutic potential.

Acknowledgments We are grateful to Ms. Sayuri Yamaguchi, Yuko Sato, and Yukari Hara for their assistance in establishing the hybridomas. We also thank Dr. Le Mai Thi Quynh at the National Institute of Hygiene and Epidemiology, Vietnam for supplying the A/Vietnam/1194/2004 virus and Dr. John Wood at NIBSC for providing the NIBRG-14 virus.

This work was supported by grants from the Ministry of Health, Labour and Welfare of Japan and from Health Science Foundation of Japan.

Conflict of interest None to declare.

REFERENCES

1. Chan, M.C., Cheung, C.Y., Chui, W.H., et al. (2005): Proinflammatory cytokine responses induced by influenza A (H5N1) viruses in primary human alveolar and bronchial epithelial cells. Respir. Res., 6, 135.
2. World Health Organization Global Influenza Program Surveillance Network (2005): Evolution of H5N1 avian influenza viruses in Asia. Emerg. Infect. Dis., 11, 1515-1521.
3. Webster, R.G. and Govorkova, E.A. (2006): H5N1 influenza—continuing evolution and spread. N. Engl. J. Med., 355, 2174-2177.
4. Webster, R.G., Guan, Y., Peiris, M., et al. (2002): Characterization of H5N1 influenza viruses that continue to circulate in geese in southeastern china. J. Virol., 76, 118-126.
5. World Health Organization: Online at 〈http://www.who.int/csr/disease/avian_influenza/country/cases_table_2011_2008_2019/en/index.html〉.
6. Uyeki, T.M. (2009): Human infection with highly pathogenic avian influenza A (H5N1) virus: review of clinical issues. Clin. Infect. Dis., 49, 279-290.

7. Gambotto, A., Barratt-Boyes, S.M., de Jong, M.D., et al. (2008): Human infection with highly pathogenic H5N1 influenza virus. Lancet, 371, 1464–1475.
8. Abdel-Ghafar, A.N., Chotpitayasunondh, T., Gao, Z., et al. (2008): Update on avian influenza A (H5N1) virus infection in humans. N. Engl. J. Med., 358, 261–273.
9 de Jong, M.D., Simmons, C.P., Thanh, T.T., et al. (2006): Fatal outcome of human influenza A (H5N1) is associated with high viral load and hypercytokinemia. Nat. Med., 12, 1203–1207.
10. Centers for Disease Control and Prevention: Seasonal Influenza (Flu). Influenza Diagnostic Testing Algorithm. Online at 〈http: // www.cdc.gov / flu / professionals / diagnosis / testing_ algorithm.htm〉.
11. Wright, P.F., Neumann, G. and Kawaoka, Y. (2007): Orthomyxoviridae. Lippincott Williams & Wilkins, Philadelphia.
12. World Health Organization: Influenza Continuing Progress towards a Unified Nomenclature System for the Highly Pathogenic H5N1 Avian Influenza Viruses. Online at 〈http://www.who.int/influenza/resources/documents/h5n1_nomenclature/en/〉.
13. Takahashi, Y., Hasegawa, H., Hara, Y., et al. (2009): Protective immunity afforded by inactivated H5N1 (nibrg-14) vaccine requires antibodies against both hemagglutinin and neuraminidase in mice. J. Infect. Dis., 199, 1629–1637.
14. Kozbor, D. and Roder, J.C. (1984): In vitro stimulated lymphocytes as a source of human hybridomas. Eur. J. Immunol., 14, 23–27.
15. Storch, G.A. (2001): Diagnostic virology. p. 493–531. Lippincott Williams & Wilkins, Philadelphia.
16. Ohnishi, K., Sakaguchi, M., Kaji, T., et al. (2005): Immunological detection of severe acute respiratory syndrome coronavirus by monoclonal antibodies. Jpn. J. Infect. Dis., 58, 88–94.
17. Graves, P.N., Schulman, J.L., Young, J.F., et al. (1983): Preparation of influenza virus subviral particles lacking the HA1 subunit of hemagglutinin: unmasking of cross-reactive HA2 determinants. Virology, 126, 106–116.
18. Russ, G., Polakova, K., Kostolansky, F., et al. (1987): Monoclonal antibodies to glycopolypeptides HA1 and HA2 of influenza virus haemagglutinin. Acta Virol., 31, 374–386.
19. Kashyap, A.K., Steel, J., Oner, A.F., et al. (2008): Combinatorial antibody libraries from survivors of the Turkish H5N1 avian influenza outbreak reveal virus neutralization strategies. Proc. Natl. Acad. Sci. USA, 105, 5986–5991.
20. Throsby, M., van den Brink, E., Jongeneelen, M., et al. (2008): Heterosubtypic neutralizing monoclonal antibodies cross-protective against H5N1 and H1N1 recovered from human IGM$^+$ memory B cells. PLoS One, 3, e3942.
21. Sui, J., Hwang, W.C., Perez, S., et al. (2009): Structural and functional bases for broad-spectrum neutralization of avian and human influenza A viruses. Nat. Struct. Mol. Biol., 16, 265–273.
22. Ekiert, D.C., Bhabha, G., Elsliger, M.A., et al. (2009): Antibody recognition of a highly conserved influenza virus epitope. Science, 324, 246–251.
23. Corti, D., Suguitan, A.L., Jr., Pinna, D., et al. (2010): Heterosubtypic neutralizing antibodies are produced by individuals immunized with a seasonal influenza vaccine. J. Clin. Invest., 120, 1663–1673.
24. Wrammert, J., Koutsonanos, D., Li, G.M., et al. (2011): Broadly cross-reactive antibodies dominate the human B cell response against 2009 pandemic H1N1 influenza virus infection. J. Exp. Med., 208, 181–193.
25. Palese, P. and Shaw, M.L. (2007): Orthomyxoviridae: the viruses and their replication. p. 1647. Lippincot Williams & Wilkins, Philadelphia.
26. Imai, M., Ninomiya, A., Minekawa, H., et al. (2007): Rapid diagnosis of H5N1 avian influenza virus infection by newly developed influenza H5 hemagglutinin gene-specific loop-mediated isothermal amplification method. J. Virol. Methods, 141, 173–180.
27. Wei, H.L., Bai, G.R., Mweene, A.S., et al. (2006): Rapid detection of avian influenza virus a and subtype H5N1 by single step multiplex reverse transcription-polymerase chain reaction. Virus Genes, 32, 261–267.
28. He, Q., Velumani, S., Du, Q., et al. (2007): Detection of H5 avian influenza viruses by antigen-capture enzyme-linked immunosorbent assay using H5-specific monoclonal antibody. Clin. Vaccine Immunol., 14, 617–623.

Biologicals 40 (2012) 96–99

Contents lists available at SciVerse ScienceDirect

Biologicals

journal homepage: www.elsevier.com/locate/biologicals

Application of deglycosylation to SDS PAGE analysis improves calibration of influenza antigen standards

Ruth Harvey [a], Michelle Hamill [b], James S. Robertson [a], Philip D. Minor [a], Galina M. Vodeiko [c], Jerry P. Weir [c], Hitoshi Takahashi [d], Yuichi Harada [d], Shigeyuki Itamura [d], Pearl Bamford [e], Tania Dalla Pozza [e], Othmar G. Engelhardt [a,*]

[a] Division of Virology, National Institute for Biological Standards and Control, Health Protection Agency, Blanche Lane, South Mimms, Potters Bar, Hertfordshire EN6 3QG, United Kingdom
[b] BioStatistics, National Institute for Biological Standards and Control, Health Protection Agency, Blanche Lane, Potters Bar, Hertfordshire EN6 3QG, United Kingdom
[c] Division of Viral Products, Center for Biologics Evaluation and Research (CBER), Food and Drug Administration (FDA), Bethesda, MD 20892, USA
[d] Center for Influenza Virus Research, National Institute of Infectious Diseases, Gakuen 4-7-1, Musashimurayama-shi, Tokyo 208 0011, Japan
[e] Therapeutic Goods Administration, PO Box 100, Woden ACT 2606, Australia

ARTICLE INFO

Article history:
Received 23 September 2011
Received in revised form
21 November 2011
Accepted 20 December 2011

Keywords:
Influenza
Vaccine
Standardisation
HA
Standards
Deglycosylation
Calibration

ABSTRACT

Each year the production of seasonal influenza vaccines requires antigen standards to be available for the potency assessment of vaccine batches. These are calibrated and assigned a value for haemagglutinin (HA) content. The calibration of an antigen standard is carried out in a collaborative study amongst a small number of national regulatory laboratories which are designated by WHO as Essential Regulatory Laboratories (ERLs) for the purposes of influenza vaccine standardisation. The calibration involves two steps; first the determination of HA protein in a primary liquid standard by measurement of total protein in a purified influenza virus preparation followed by determination of the proportion of HA as determined by PAGE analysis of the sample; and second, the calibration of the freeze-dried reference antigen against the primary standard by single radial immunodiffusion (SRD) assay. Here we describe a collaborative study to assess the effect of adding a deglycosylation step prior to the SDS-PAGE analysis for the assessment of relative HA content. We found that while the final agreed HA value of the samples tested was not significantly different with or without deglycosylation, the deglycosylation step greatly improved between-laboratory agreement.

1. Introduction

Vaccination against seasonal and pandemic influenza virus remains an important strategy to reduce morbidity and mortality associated with the disease [1]. Inactivated seasonal trivalent vaccines produced by numerous manufacturers worldwide currently contain standardized amounts of the haemagglutinin (HA) from an A/H1N1, A/H3N2 and B strain of influenza virus. Due to rapid mutation in influenza viruses (antigenic drift), the World Health Organisation (WHO) makes biannual recommendations for the strains to be used in the formulation of influenza vaccine, based on worldwide surveillance and characterisation of circulating strains [2]; as a result, one or more strains in the vaccine typically needs to be updated (reviewed in [3] and [4]). The potency of each lot of vaccine produced is determined by the single radial immunodiffusion assay (SRD) which has been the WHO recommended assay for influenza vaccine potency determination since 1979 [5,6]. The use of SRD for quantitation of HA antigen in vaccine requires a set of two reference reagents, an HA antigen standard and an anti-HA sheep antiserum, that match the vaccine strain. Thus, new reagents must be prepared each time there is a change in the WHO recommended vaccine strain.

The anti-HA sheep antiserum is raised against purified HA from the recommended strain. The HA antigen reagent is typically a preparation of inactivated whole virus donated by a vaccine manufacturer that is freeze-dried by, or on behalf of, an Essential Regulatory Laboratory (ERL). To calibrate this reagent, a primary liquid standard (PLS) is prepared by an ERL from a purified virus preparation of the recommended strain. The total protein within a PLS is determined using a standard protein quantitative assay (e.g. Lowry) whilst the proportion of HA protein within the PLS is determined from a densitometric analysis of the viral proteins separated by SDS-PAGE run under both reduced and non-reduced conditions [7]. In this assay it is the protein bands of the reduced samples that are used in the quantitation, with the non-reduced

* Corresponding author. Tel.: +44 01707 641000; fax: +44 01707 641366.
E-mail address: othmar.engelhardt@nibsc.hpa.org.uk (O.G. Engelhardt).

1045-1056/$36.00
doi:10.1016/j.biologicals.2011.12.009

samples run alongside to aid in identification of the protein bands where a degree of co-migration occurs. Densitometric analysis of protein bands in the non-reduced samples is not optimal for accurate quantitation because a lot of the proteins co-migrate or are present as higher molecular weight aggregates.

The calibration of a PLS is performed in a collaborative study within WHO designated ERLs, namely the Centre for Biologics Evaluation and Research (CBER), Food and Drug Administration, USA, the National Institute for Biological Standards and Control (NIBSC), Health Protection Agency, UK, the National Institute of Infectious Diseases (NIID), Japan and the Therapeutic Goods Administration (TGA), Australia. The data from all laboratories are collated so that an HA content value in μg can be assigned to the PLS. The primary standard is then used in SRD to calibrate the freeze-dried secondary standard, which is the antigen reference material used by manufacturers as well as National Control Laboratories for the potency testing of an influenza vaccine.

Quantitation of peaks from the densitometric analysis of the SDS-PAGE of purified virus preparations is sometimes technically challenging due to various degrees of co-migration of the relevant protein bands. This phenomenon is strain-dependent and not predictable. Recently we described a modification of the SDS-PAGE method to include deglycosylation of samples before analysis [8]. Because deglycosylation shifts the mobility of the HA bands within the SDS-PAGE gels, this modification improved the reproducibility of the quantitation of the HA in our laboratory. Therefore, a collaborative study was set up among the ERLs to assess the modified method in comparison to standard in-house methods of the ERLs for the calibration of HA antigen reagent.

2. Materials and methods

2.1. Study design

A panel of purified preparations of four viruses was sent to each of the four ERLs. Each laboratory tested the samples for HA content (% HA) using their standard in-house methodology and then tested the samples following a prescribed method for the deglycosylation method. Data was returned to NIBSC, collated and statistical analysis carried out to assess the reproducibility of the alternative methods within and between laboratories. Each sample was tested by each laboratory by each method at least three times, so all data shown are the average of at least 3 individual data points.

2.2. Virus concentrates

A panel of viruses was made comprised of PR8 (H1N1), NYMC X-157 (H3N2), NYMC X-161b (H3N2) and IVR-116 (H1N1). All viruses were grown in 11 day old embryonated hens' eggs. Allantoic fluid was harvested 72 h post infection and was clarified at high speed (10 000 rpm, 30 min, 4 °C, in a Beckman SW28 rotor). Virus was pelleted by centrifugation (25 000 rpm, 90 min at 4 °C in a Beckman SW28 rotor). Virus pellets were resuspended in 1 ml PBS and loaded onto an 11 ml, 10–40% continuous sucrose gradient which was centrifuged at 35 000 rpm for 35 min at 4 °C in a Beckman SW41 rotor. The virus band was harvested, made up to an appropriate volume in PBS, pelleted by centrifugation (25 000 rpm, 90 min, 4 °C, in Beckman SW28 rotor) and the final virus pellet resuspended in PBS (10 μl per egg used).

2.3. SDS-PAGE analysis

SDS-PAGE analysis was performed in each laboratory according to standard protocols. For the gel in Fig. 1 the following method was used. One to 3 μL of virus concentrate (approximately 10 μg total protein) was mixed with water to a total volume of 10 μl. Loading dye (2.5 μl) with 2% (v/v) β-mercaptoethanol as reducing agent was added to each sample. Samples were heated to 95 °C for 3 min prior to loading onto the gels. Ten percent Bis-Tris gels were used and run at 125 V for 90 min using MOPS buffer (Invitrogen) followed by staining using Colloidal Blue stain (Invitrogen). Quantitation was carried out using an Imagescanner and associated software (GE healthcare). The content of HA for each sample was calculated as follows; firstly, the total viral protein value, in arbitrary units, was calculated by summing the quantitated values for the HA1, HA2, NP and M1 bands on the gel (these were the predominant bands observed in the SDS-PAGE gels of purified virus). The HA1 and HA2 values were summed to give the total HA value. The percent HA of total protein was calculated by dividing the total HA by the total protein multiplied by 100.

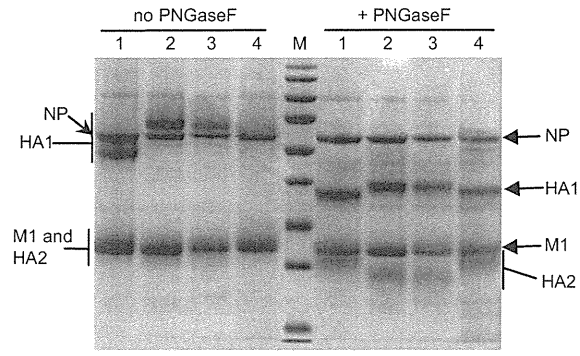

Fig. 1. SDS PAGE analysis of viruses. The four viruses included in the panel to be tested by each laboratory were analysed by SDS PAGE. Sample 1, PR8; 2, NYMC X-157; 3, NYMC X-161b; 4, IVR-116. All virus samples were reduced. Viruses were compared either deglycosylated (PNGase F +), or non deglycosylated (PNGase F -).

2.4. Deglycosylation using PNGase F

Deglycosylation was achieved using PNGase F (New England Biolabs). Approximately 10 μg (typically 1–3 μl) of each virus concentrate was denatured according to the PNGase F manufacturer's instructions in a total reaction volume of 10 μl and samples were incubated at 37 °C overnight (approx. 16 h) with 1 μl of a 1/20 dilution of PNGase F enzyme in buffer provided by the manufacturer and 1% final concentration NP40 (provided with enzyme). Loading dye (2.5 μl) with 2% (v/v) β-mercaptoethanol as reducing agent was added to each sample. Samples were heated to 95 °C for 3 min prior to loading onto SDS-PAGE gels. Gels were run and stained as above.

2.5. Statistical analysis

Statistical analysis was performed using Minitab 15 statistical software. The analysis was performed using a general linear model with the Tukey method for pair-wise comparisons [9].

3. Results

A panel of seasonal viruses was assembled and assessed by SDS PAGE analysis with and without deglycosylation (Fig. 1). The results show that when the virus samples are run under reducing conditions with no PNGaseF treatment, there are varying degrees of co-migration between the viral protein bands. Of note, the NA protein often cannot be seen on gels, as there is not enough present to produce a visible band and, as a glycoprotein, it is diffuse without deglycosylation. When deglycosylation is used, a discrete NA band may be apparent for some viruses, but, as observed in this study,

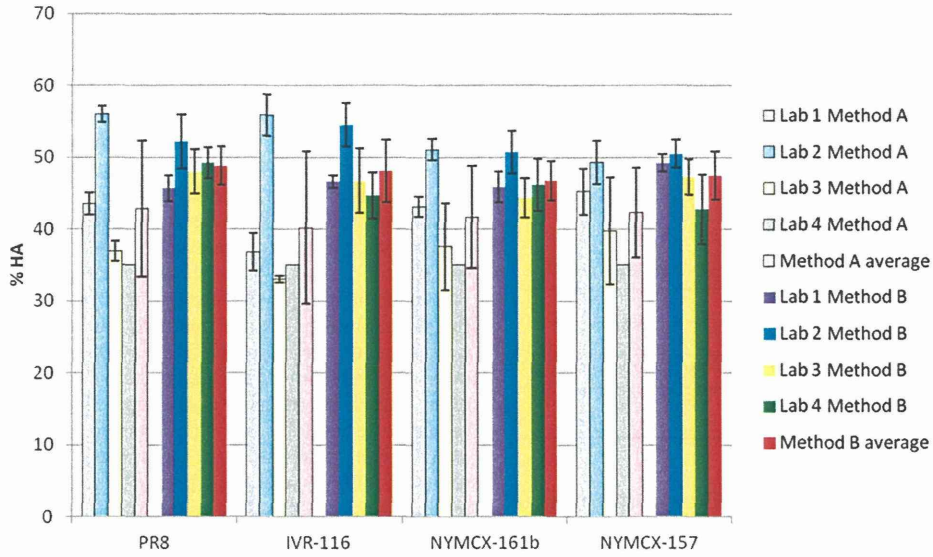

Fig. 2. HA content of viruses. Each of the four laboratories measured HA content using their in-house method (Method A) or the prescribed deglycosylation protocol (Method B). Results shown are the average of ≥3 separate experiments for each method and each sample, except for lab 4 Method A as explained in the text. The overall average for each virus/method is also shown (average). Error bars denote standard deviations.

this is not always the case. Running the same set of virus samples under reducing conditions after deglycosylation leads to much better separation of the viral proteins, which allows more accurate and reproducible quantitation.

We analysed %HA values with (method B) or without (method A) deglycosylation treatment of samples, based on the original in-house SDS-PAGE procedures of each laboratory. In order to compare the reproducibility of the methods among laboratories a single method for calculating the %HA content as described in materials and methods was used. One participant, laboratory 4, did not have an in-house experimental method for the quantitation of %HA and uses an assumed value of 35% instead, based on historical experience for assignment of HA content to the PLS. Therefore, no method A was included in the statistical analysis for laboratory 4, but an assumed value 35% is included in the results of the study shown in Fig. 2.

Tables 1 (method A) and 2 (method B) show individual means for each method, lab and virus calculated using data from replicate responses, expressed as %HA protein of the total viral protein in a sample. Overall means for each lab were calculated as the mean of the four individual virus means within the lab, and overall means for each virus were calculated as the mean of the individual lab means for each of the viruses.

The results for all viruses were similar for both methods, with an overall mean of 44%HA for method A and a mean of 48%HA for method B.

Within a virus, variability between labs depended on the method, with method B appearing to have better agreement between labs than method A. This is reflected by the between lab CV for individual viruses, which ranged from 10% to 30% for method A and 5%–9% for method B. Similarly, the overall between lab variability was lower for method B than for method A (6% and 19% respectively), indicating an overall improved agreement between labs for method B as compared to method A.

Between replicate variability (Tables 3 and 4) was assessed by pooling individual CVs calculated from replicate responses within each lab and virus. Estimates were pooled both across viruses within a lab to give a pooled estimate of within lab, between replicate variation, and across labs within a virus to give a pooled estimate of within virus, between replicate variation. An overall pooled estimate of between replicate variability for each method was calculated using the average of the pooled standard deviations and the overall mean for the particular method.

Overall pooled estimates for both methods were similar (7.0% for method A and 5.8% for method B) indicating similar between replicate variability for the two methods.

For method A, pooled CVs within a lab and virus were less than 10%, with the exception of lab 3 which was marginally more variable at 13.6%. This was due to two viruses, NYMC X-161b and NYMC X-157 which had higher between replicate variability (16.1% and 18.6% respectively) than viruses PR8 and IVR-116 (3.9% and 1.3% respectively). This is reflected also by the pooled within virus CVs which are higher for NYMC X-161b and NYMC X-157 (9.1% and 9.4%) than for PR8 and IVR-116 (3.5% and 5.9%). Comparing the pooled within lab CVs and the between virus CVs (Tables 1 and 3) and taking into

Table 1
Method A lab and virus means with between-lab %CVs.

Virus	Method A			Virus mean	Between lab %CV
	Lab 1	Lab 2	Lab 3		
IVR-116	36.85	55.88	33.02	**41.92**	**29.21**
NYMC X-157	45.21	49.32	39.76	**44.76**	**10.71**
NYMC X-161b	43.10	51.07	37.56	**43.91**	**15.47**
PR8	43.57	56.00	36.96	**45.51**	**21.24**
Lab Mean	**42.18**	**53.07**	**36.83**	**44.03 (overall)**	**18.80**

Values shown are the averages of at least 3 independent experiments.
Bold indicates means between viruses and/or labs, as well as CVs.

Table 2
Method B lab and virus means with between-lab %CVs.

Virus	Method B				Virus mean	Between lab %CV
	Lab 1	Lab 2	Lab 3	Lab 4		
IVR-116	46.62	54.46	46.72	44.67	**48.12**	**9.00**
NYMC X-157	49.23	50.46	47.31	42.81	**47.45**	**7.07**
NYMC X-161b	45.87	50.67	44.37	46.09	**46.75**	**5.82**
PR8	45.73	52.16	48.44	49.19	**48.88**	**5.41**
Lab Mean	**46.86**	**51.94**	**46.71**	**45.63**	**47.79 (overall)**	**5.91**

Values shown are the averages of at least 3 independent experiments.
Bold indicates means between viruses and/or labs, as well as CVs.

Table 3
Method A pooled CVs (within lab and within virus – based on replicate tests).

Method A						
Lab			Virus			
1	2	3	IVR-116	NYMC X-157	NYMC X-161b	PR8
5.46	4.72	13.55	5.93	9.38	9.11	3.50
7.02						

Table 4
Method B Pooled CVs (within lab and within virus – based on replicate tests).

Method B							
Lab				Virus			
1	2	3	4	IVR-116	NYMC X-157	NYMC X-161b	PR8
3.53	5.84	6.10	7.90	6.14	5.71	6.32	5.54
5.75							

account the range of variability between replicates in lab 3, there is no evidence to suggest that the variability between viruses is anything more than assay variation. However, the pooled within virus CVs are much lower (3.5%–9.4%) than the between lab CVs (10%–30% from Table 1), suggesting that the variability between labs for method A is greater than assay variation alone. This was confirmed by two-way analysis of variance where all labs were significantly different from all other labs ($p < 0.001$ in all cases).

For method B, all pooled CVs were less than 10% and were comparable with the between lab and between virus figures from Table 2 indicating that the %CVs from Table 2 are similar to assay variation. However, a two-way analysis of variance showed the mean for lab 2 to be higher than all other labs; although the difference in means was small, it was statistically significant ($p < 0.001$). No significant differences were found between any other labs ($p > 0.05$ in all cases).

From the data provided, both methods A and B give similar overall mean %HA results (44%, Table 1, and 48%HA, Table 2, respectively). Overall assay variation, as measured by the overall pooled %CV's was similar for both methods. The variability between viruses was low for both methods and comparable with between replicate variability, however method B showed improved agreement between labs compared to method A.

4. Conclusion

We have previously demonstrated that a modification of the SDS-PAGE method to include deglycosylation of samples before analysis improved the reproducibility of the quantitation of the HA of H5N1 viruses in our laboratory [8]. A study by Li et al. [10] also showed that the modified method led to very reproducible data for HA content (% HA) in pandemic H1N1 viruses. Here we have demonstrated that the new protocol for determination of HA content, which involves deglycosylation of the samples prior to running SDS-PAGE, improved the agreement between the laboratories participating in the study. The study involved 4 ERL laboratories assessing the HA content for a panel of seasonal influenza viruses using their current standard in-house method and the new prescribed method for deglycosylation. The overall results for percentage HA content, while displaying a trend towards slightly higher HA content values, were not statistically significantly changed by use of the modified method, which is a reflection of the robustness of the methods currently used; however, a move towards even closer agreement between the results generated is a significant improvement. This study was carried out using a small selection of seasonal influenza A virus samples. The level of glycosylation can vary (significantly) between different influenza viruses and so it may be found in the future that this method is even more useful for particularly problematic viruses. For example, some H5N1 strains have been shown previously [8] to have a significant problem of co-migration of proteins due to the level of glycosylation of the HA. It may be of value to continue the comparison of currently used methods alongside the deglycosylation protocol during the calibration of reference reagents over a number of influenza seasons to obtain more data and to fully assess the suitability of such a method for the calibration of reagents in the future. The deglycosylation step may need to be optimised for each new strain at the start of a season as we have seen some differences between viruses in the sensitivity to the PNGase F enzyme, with some viruses requiring longer periods of treatment, or more enzyme in the reaction (data not shown). In the future we can also investigate ways to improve agreement for the total protein determination, which is the other part of the collaborative process for calibration of potency reference reagents. There is potential to optimise this part of the assay as well as the HA quantitation procedure and so improve the reproducibility of calibration further. In the future it might be worth investigating the standardisation of SDS-PAGE gel consumables, equipment and protocols as well as standardisation of the quantitation procedure between the ERLs; however, as the present study shows, this is not needed urgently. Other physicochemical methods such as mass spectrometry can also be used to measure the absolute amount of a protein in a sample; ultimately a method such as this may be even more accurate. However, a lot of assay development and validation would be required before a new method like that could be employed, and a method like mass spectrometry requires more expertise and specific equipment, so it may be some time before it could be used routinely in all ERLs. Overall this study shows that the new method is more reproducible and thus has the potential to improve the calibration of influenza reference antigen reagents.

Acknowledgements

This work was funded in part by an MRC grant (number G0600509) awarded to Dr J.S. Robertson. We would like to thank Robert Newman for providing the panel of virus concentrates.

References

[1] Germann TC, Kadau K, Longini IM, Macken CA. Mitigation strategies for pandemic influenza in the United States. PNAS 2006;103:5935–40.
[2] Russell CA, Jones TC, Barr IG, Cox NJ, Garten RJ, Gregory V, et al. Influenza vaccine strain selection and recent studies on the global migration of seasonal influenza viruses. Vaccine 2008;26S:D31–4.
[3] Tosh PK, Jacobson RM, Poland GA. Influenza vaccines: from surveillance through production to protection. Mayo Clin Proc 2010;85(3):257–73.
[4] Orenstein WA, Schaffner W. Lessons Learned: Role of influenza vaccine production, distribution, supply and demand – What it means for the provider. Am J Med 2008;121:S22–7.
[5] Wood JM, Schild GC, Newman RM, Seagroatt V. An improved single-radial-immunodiffusion technique for the assay of influenza haemagglutinin antigen: application for the potency determinations of inactivated whole virus and subunit vaccines. J Biol Stand 1977;5:237–47.
[6] WHO. WHO Expert committee on Biological Standardization. Thirteenth report. Geneva: World Health Organisation; 1979. Annex 3 (WHO Technical Report Series, No. 638).
[7] Wood JM, Mumford JA, Dunleavy U, Seagroatt V, Newman RW, Thornton D, et al. Single radial immunodiffusion potency tests for inactivated equine influenza vaccines. In: Powell DG, editor. Equine infection disease V. Proc. Fifth International Conference. Kentucky: The University Press; 1988. p. 74–9.
[8] Harvey R, Wheeler JX, Wallis CL, Robertson JS, Engelhardt OG. Quantitation of haemagglutinin in H5N1 influenza viruses reveals low haemagglutinin content of vaccine virus NIBRG-14 (H5N1). Vaccine 2008;26:6550–4.
[9] Hsu JC. Multiple comparisons, Theory and methods. Chapman and Hall; 1996.
[10] Li C, Shao M, Cui X, Song Y, Li J, Yuan L, et al. Application of deglycosylation and electrophoresis to the quantification of influenza viral hemagglutinins facilitating the production of 2009 pandemic influenza (H1N1) vaccines at multiple manufacturing sites in China. Biologicals 2010;38:284–9.